SIM.EM-K3
Key Comparison of 10 mH Inductance Standards at 1 kHz

FINAL REPORT

February 2016

José Angel Moreno Hernández
Centro Nacional de Metrología, Mexico.

SIM.EM-K3
Key Comparison of 10 mH Inductance Standards at 1 kHz

FINAL REPORT

Contents

1. Introduction

To strengthen the Interamerican Metrology System (SIM), a key comparison of reference standards of measurement among its National Metrology Institutes (NMI's) is promoted. At the same time, in accordance with the CIPM Mutual Recognition Arrangement (MRA) objectives, NMI´s must establish the degree of equivalence between their national measurement standards by performing regional comparisons, among other activities. With this view, a Key Comparison of 10 mH Inductance Standards at 1 kHz was organized with the participation of seven NMI's from the SIM Regional Metrology Organization.

The objective of this comparison was to compare the measurement capabilities of NMIs in SIM in the field of inductance, determining the degree of equivalence of the measurement results.

2. Organization

2.1. Participants

Seven NMIs participated in the comparison:

- Administración Nacional de Usinas y Trasmisiones Eléctricas (UTE) – Uruguay
  Contact person: Daniel Izquierdo.

- Centro Nacional de Metrología (CENAM) – Mexico
  Contact person: José Ángel Moreno.

- Instituto Costarricense de Electricidad (ICE) - Costa Rica
  Contact person: Blanca Isabel Castro.

- Instituto Nacional de Metrologia, Qualidade e Tecnologia (INMETRO) – Brazil
  Contact person: Renata de Barros e Vasconcellos.

- Instituto Nacional de Tecnología Industrial (INTI) – Argentina
  Contact person: Marcelo Cazabat.

- National Institute of Standards and Technology (NIST) - United States of America
  Contact person: Andrew Koffman.

- National Research Council (NRC) – Canada
  Contact person: Marcel Cote.

2.2. Coordinator and Support Group

This comparison was coordinated by CENAM (Jose Angel Moreno) as Pilot Laboratory. The support group was integrated by NRC (Carlos Sánchez) and INMETRO (Gregory Kyriazis).

2.3. Schedule of Measurements

The circulation of the traveling standards was arranged in three short loops having a close surveillance of the value of the standards during its transportation from one to other NMI.

Different situations caused departures from the original schedule of the comparison, for example long time bureaucratic procedures in customs, holydays periods and review of the traveling standards after transport, always with the priority of not to expose the traveling standards and accessories to adverse conditions, and avoiding unnecessary delays.

Table 1 shows the period of stay of the traveling standards at each laboratory, according the confirmation of Dispatch and Receipt issued by the participants.

Table 1 Period of stay of traveling standards during the SIM.EM-K3 comparison.

NMI	Period
CENAM	2013-June-07 to 2013-September-09
NRC	2013-September-19 to 2013-October-29
NIST	2013-November-05 to 2014-January-13
CENAM	2014-January-31 to 2014-March-05
INTI	2014-April-03 to 2014-June-11
INMETRO	2014-July-17 to 2014-August-22
CENAM	2014-September-17 to 2014-October-29
ICE	2014-November-20 to 2015-January-20
UTE	2015-February-20 to 2015-April-09
CENAM	2015-April-16 to 2015-May-08

3. Traveling Standards

From previous experiences it is known that standard inductors are sensitive to transport effects. In order to evaluate and take in consideration of such effects during the comparison, three reference standards were used, two of them are property of NIST and one of NRC. Additionally, CENAM provided its own reference group of four standards and a measuring system based on a Maxwell-Wien bridge, which allows a continued record of measurements since 2005, in order to provide a close surveillance of the traveling standards during the transport and stay at each participant NMI. Table 2 shows the details of the traveling standards used in the comparison.

Table 2 Traveling standards used in the SIM.EM-K3 comparison.

Id.	Manufacturer	Model	Serial
L_5	General Radio Company	1482-H	7270
L_6	General Radio Company	1482-H	19782
L_7	IET	1482-H	B2-11521295

Previous to start the comparison, the inductors were characterized in order to know its temperature coefficients of inductance and resistance [1], and evaluate its stability. The table 3 shows the temperature coefficients of inductance α_L and the temperature coefficients of resistance α_R for each traveling standard.

Table 3 Temperature coefficients of inductance and resistance of the traveling standards.

Id.	α_L (µH/H / °C)	α_R (mΩ/°C)
L_5	37.3 ± 1.8	32.3 ± 7.7
L_6	48.6 ± 1.6	32 ± 13
L_7	37.6 ± 1.4	33.26 ± 0.35

To minimize the effect of the temperature during the measurements, each inductor was placed in individual enclosures with controlled temperature of around 28.5 °C, powered with a 12 V power source.

The temperature of each enclosure was determined through the electrical resistance of a CENAM calibrated Pt100 sensor placed directly in one of the lateral walls of the inductor. The PT100 sensor was configured to be measured using a 4-terminal resistance meter or a thermometry bridge by means of Voltage and Current BNC connectors. All participants received from the pilot laboratory a spreadsheet to calculate the temperature of the enclosure according the parameters given in the comparison technical protocol. The expanded uncertainty of the temperature measurement is estimated to be 0.02 °C.

A battery operated Data Logger was attached to the L_5 enclosure to register temperature, humidity, pressure and tri-axial mechanical shocks during the transport.

The enclosures containing the traveling standards and all accessories were transported using a hard transport case, which was moved using forklift.

Figure 1 shows the L_5 enclosure, which shows the power source and Data Logger location, and figure 2 shows the transport case to ship the traveling standards.

Figure 1 Temperature controlled enclosure used in the SIM.EM-K3 comparison.

Figure 2 Transport case for shipping traveling standards.

Additionally, as check standards the pilot laboratory used a bank of 4 inductors having continuous records of measurements since 2005. One of these inductors was maintained in a temperature controlled enclosure having the same construction as the traveling standards used for the comparison. This bank of inductors was maintained at CENAM during the comparison and measured periodically using the same measuring system as for the official measurements.

4. Measurements and Results

4.1. Measurements during transport

During the transport of the traveling standards four different quantities were recorded by the Data Logger located on L_5 enclosure: temperature, humidity, pressure, and tri-axial shock, where X-Y-Z shock components were independently measured and the resultant shock vector is calculated. According to the location of the Data Logger, the X and Z shock components correspond to lateral to the enclosure shocks, and Y component corresponds to vertical shocks, as illustrated in figure 3.

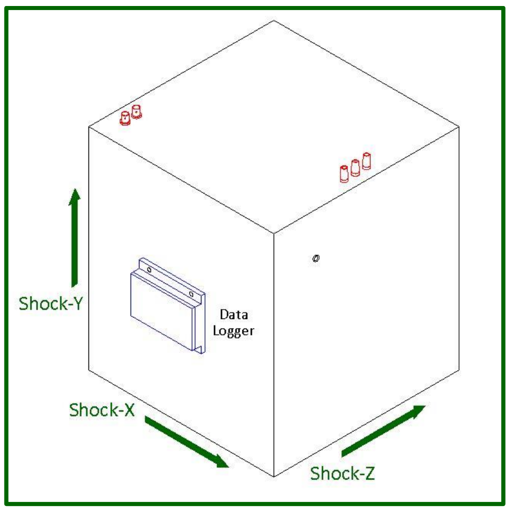

Figure 3 X-Y-Z shock components identification.

The Data Logger was configured to take measurements every 5 minutes, where the shock registered values corresponds to the higher value occurred during this period.

Each participant was requested to download the information stored by the Data Logger during the transport of the traveling standards, which was sent to the pilot laboratory. Only during the transport from NIST to CENAM it was not possible to obtain the information from the Data Logger.

During the first loop of the comparison it was observed some erratic data, that after technical reviews at CENAM it was found that the battery pack internal connections failed during customs inspections or unpacking traveling standards. The data was debugged to discard false information, and modifications to the battery pack were made.

The temperature around the traveling standards during transportation maintained in a range from 17 °C to 26 °C, where the lowest temperature was near to 5 °C occurred during the transport from NRC to NIST in November 2013 , and the highest temperature was near to 32 °C occurred during the transport from INMETRO to CENAM in September 2013. Figure 4 shows the recorder temperature during the comparison.

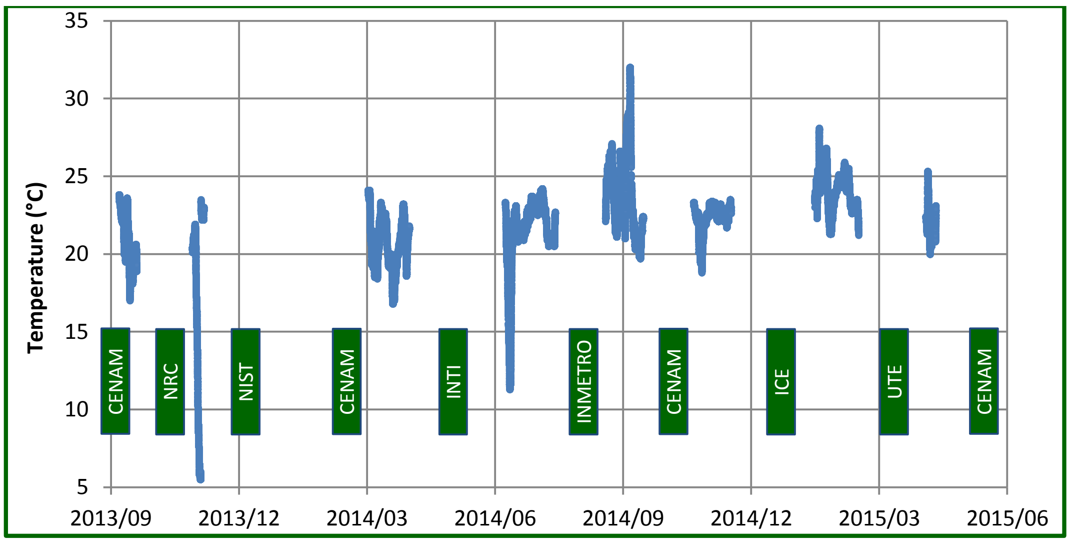

Figure 4 External temperature of L_5 during transportation.

The humidity maintained in a range from 25 % H.R. to 70 % H.R as shown in figure 5.

Figure 6 shows that the pressure was in a range from 72 kPa to 104 kPa, were is revealed that atmospheric pressure of the case is related to the altitude of each NMI or to the transfer airport during the transport.

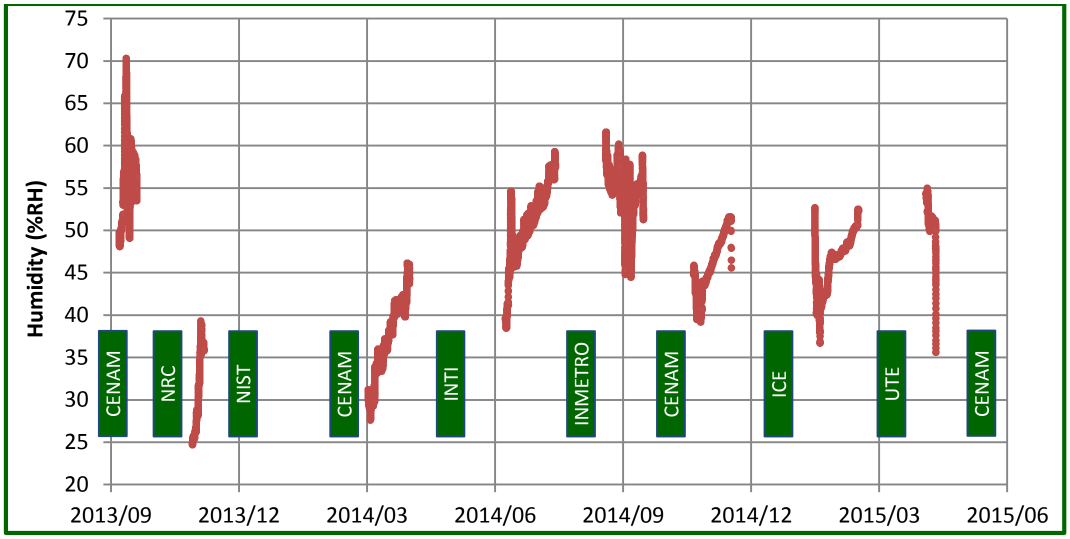

Figure 5 Internal humidity of the transport case.

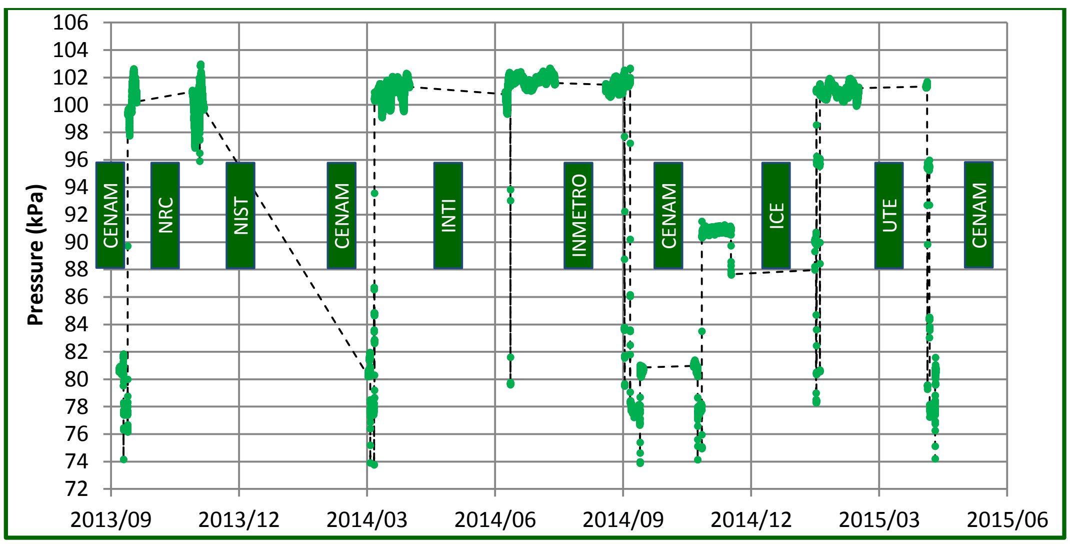

Figure 6 Internal pressure of the transport case.

Finally, shock measurements reveal that during some transportations the shocks maintained below 70 m/s^2 (≈ 7 g_n) but for most of the transports the level of shock are similar having high values near to 150 m/s^2 (≈ 15 g_n) during the CENAM-INTI, INTI-INMETRO, ICE-UTE and UTE-CENAM transportations, as can be observed in figure 7.

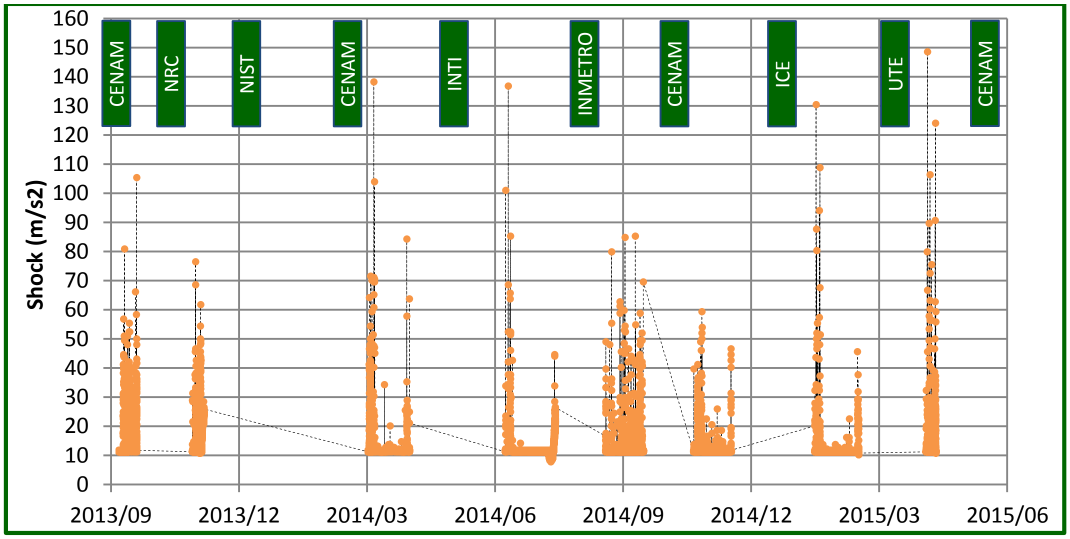

Figure 7 Shock vector during transport.

For the CENAM-INTI, ICE-UTE and UTE-CENAM transports it was detected that the major shock component occurred in the vertical direction (shock-Y), as can be observed in figure 8. This corresponds most likely to drops of the case.

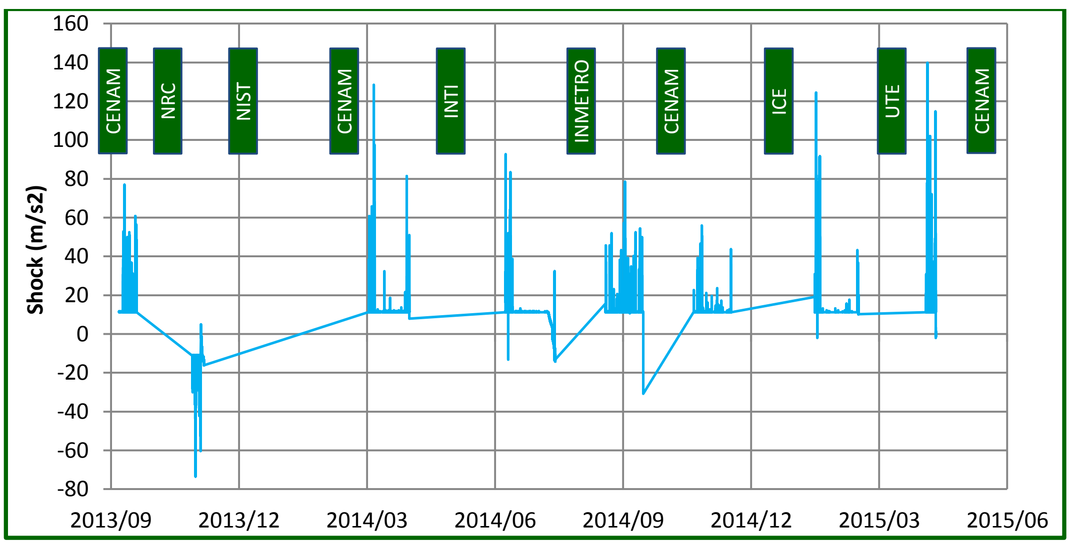

Figure 8 Shock-Y during transport.

Additionally, it was detected that the vertical shocks during the transport from NRC to NIST occurred in a negative direction. NRC and NIST confirmed that the Data Logger was positioned according the figure 3, which means that the case was transported in a vertically inverted position.

In the case of the INTI-INMETRO transportation, the major shock component corresponds to a lateral shock, as can be seen in figure 9, which could occur due to a collision with other object or even a lateral drop.

Shock in X direction maintained relative low and similar for all transportation as shown in figure 10.

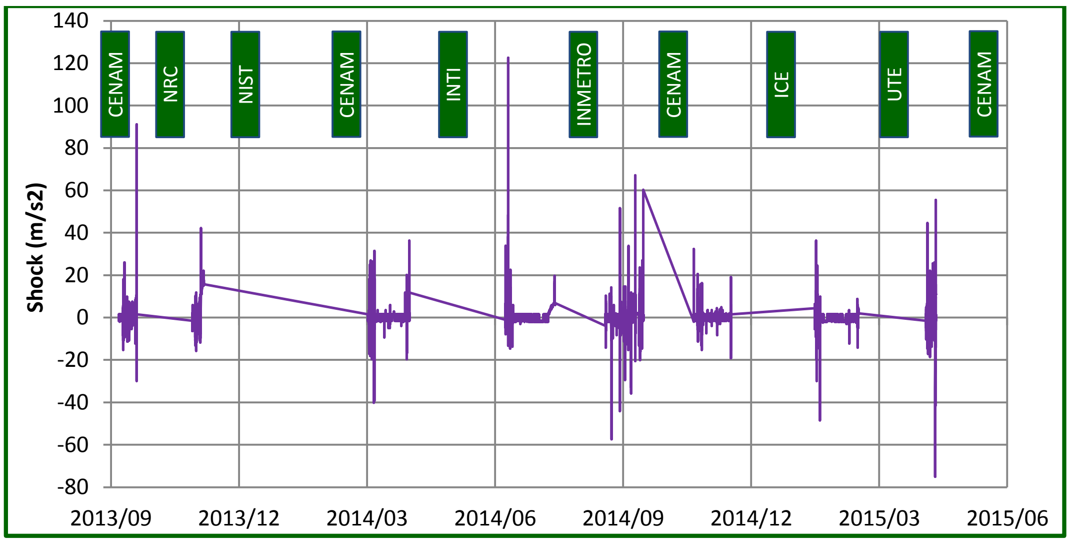

Figure 9 Shock-Z during transport.

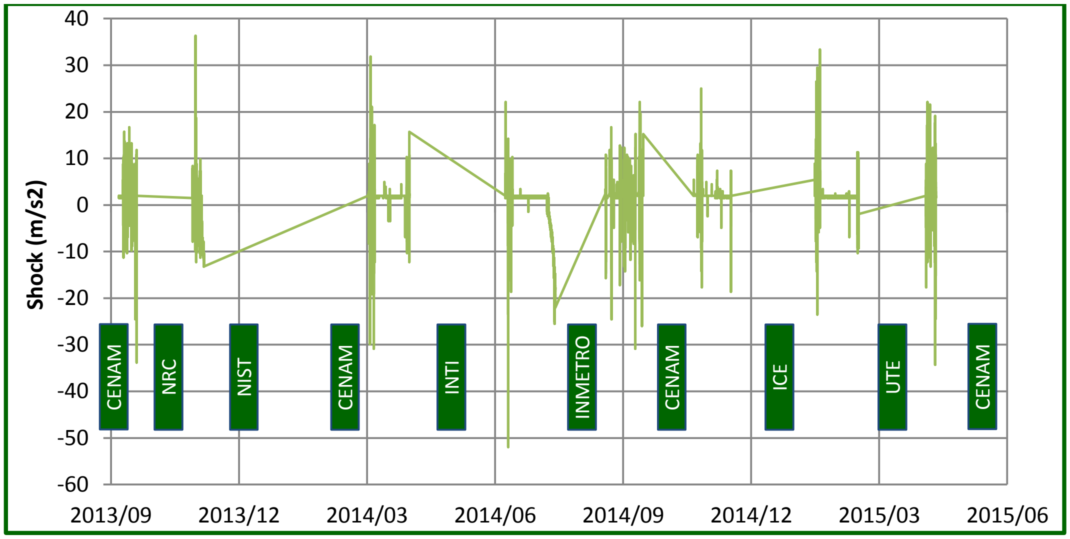

Figure 10 Shock-X during transport.

4.2. Surveillance measurements

The participants were requested to measure the inductance of the traveling standards at 1 kHz in Two-Terminal configuration in series equivalent circuit, using a maximum current of 10 mA, at the temperature of the enclosure of each traveling standard.

In order to detect transport effects which could invalidate measurements, all participants were requested to perform surveillance measurements. These measurements were made every working day after receiving the traveling standards and the enclosure temperature is stable according to the technical protocol. The Inductance measurements could be made using a RLC digital bridge with resolution of at least 1 µH/H at 1 kHz, having good practices in cables compensation, but some NMIs measured using a better measuring system.

Using the surveillance measurements they were calculated the inductance difference between the three traveling standards L_6-L_5, L_7-L_5 and L_7-L_6. It is expected that these differences should be maintained if the inductors are free of transport effect, so only one considerable change was detected during the travel from CENAM to INTI. Figure 11 shows that the difference L_6-L_5 changed about 100 µH/H. Analyzing the differences L_7-L_5 and L_7-L_6 it was detected that the inductor L_6 suffered such change, which was confirmed by means of the official measurements. Additionally, it is very clear that the observed drift of the difference L_6-L_5 changed.

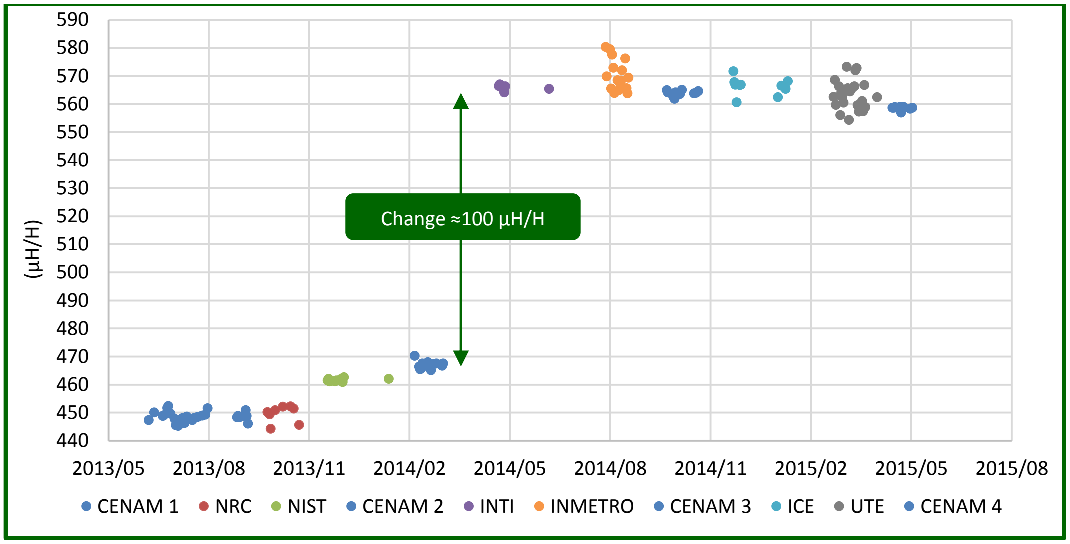

Figure 11 Surveillance difference L_6-L_5.

The reason of the detected change is not completely clear. Analyzing in detail the Data Logger information of the transport from CENAM to INTI, figure 12 shows that no big temperature of humidity cycling existed, and in figure 13 the pressure measurements do not reveal some anomalous behavior. The only possible clue is a vertical drop near to 140 m/s^2 (≈ 14 g_n) occurred just before the flight from Mexico City to Buenos Aires. Other similar drops occurred in subsequently occasions, but no changes were observed.

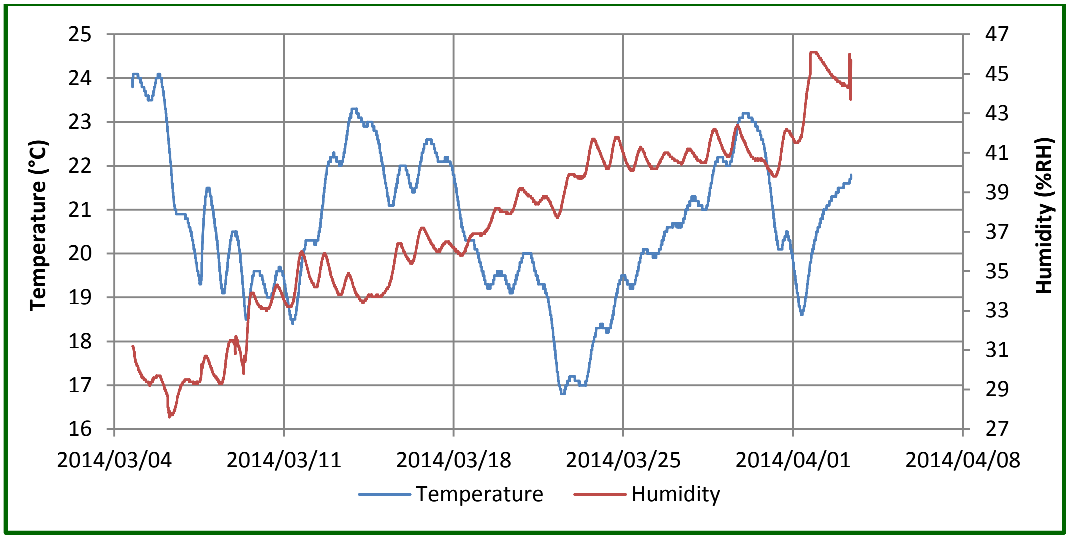

Figure 12 Temperature and Humidity measurements during CENAM-INTI transport.

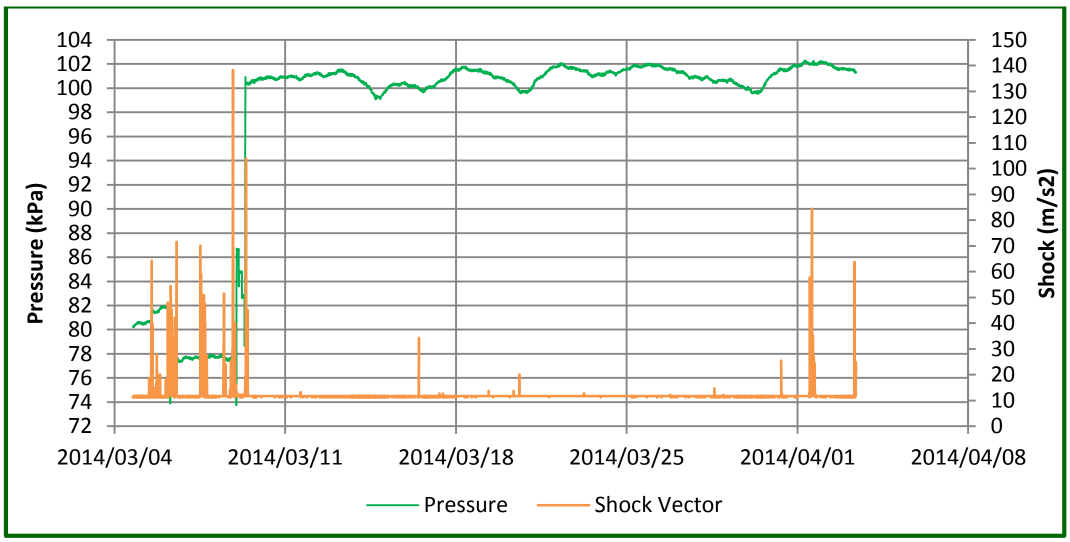

Figure 13 Pressure and Shock measurements during CENAM-INTI transport.

During the second and third loop of the comparison, it was detected that the internal connections of the inductors were damaged during some transports, where the connection from the outside terminals to the inductor terminals were broken as can be seen in figure 14.

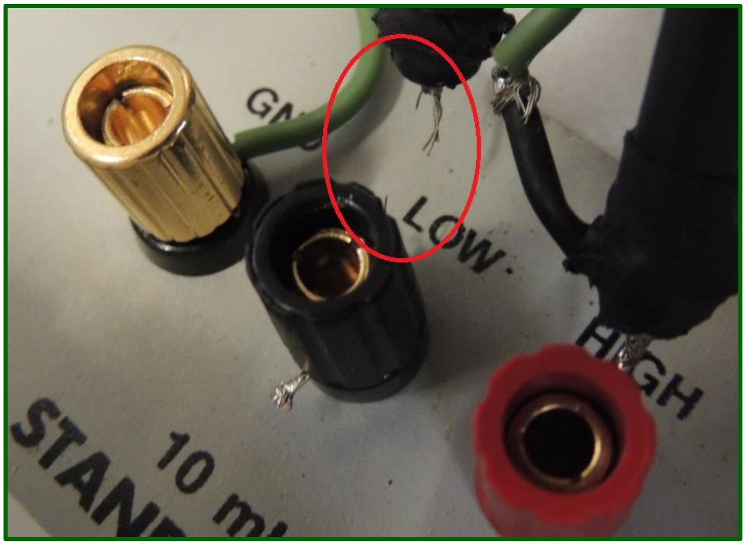

Figure 14 Damaged internal connection.

The damages were detected for the inductors L_6 and L_7 during the transport from CENAM to INTI, for the inductor L_5 during the transport from INTI to INMETRO, and for the inductor L_7 for the transport from ICE to UTE. According to the evidence, the damages were caused mainly by two factors: a) the internal foam used to support mechanically the inductors was not placed properly to avoid movements of the inductor during the transport, and b) the connectors of the inductors had edges sharp enough to damage the connecting cables.

With the support from the technical personnel of INTI, INMETRO and UTE, the connections of the inductors were fixed satisfactorily. Considering that the wires used for the repairs did not exceed the original ones by more than 1.5 cm in length and 2 mm in diameter, and the geometry did not changed drastically from a straight wire, then according to [2] it has been computed that the maximum influence of the repair is 0.6 µH/H. The surveillance or official measurements cannot reveal this influence due the dispersion of the measurements, so it can be considered that the repairs didn't have a significant effect in the results.

4.3. Official measurements and measuring systems

The participants were requested to report a minimum of 8 individual official measurements along 8 different days, to be reported to the pilot laboratory within six weeks after completing the measurements. The information to be reported includes:

- Date of measurements.
- Ambient temperature and humidity.
- Output voltage of the Power Source.
- Temperature of the enclosure.
- DC resistance of the traveling standard.
- Inductance of the traveling standard.

During the second loop of the comparison, just before the transport from CENAM to INTI, it was detected that the Pt100 sensor of the L_7 inductor suffered damage on its leads, as shown in figure 15.

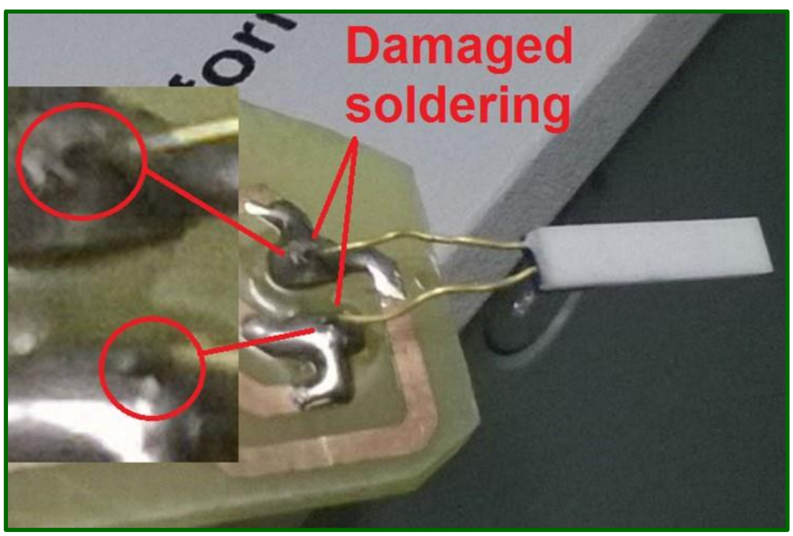

Figure 15 Damaged leads of L_7 Pt100 sensor.

Due this reason, the enclosure temperature measurements reported by INTI and INMETRO were considered invalid, which was reported to the involved laboratories. In the particular case of INMETRO, the reported temperature was around 43 °C, so it was decided to turn off the oven and measure the inductor without temperature control.

In order to estimate the L_7 temperature, it was proposed to use a different method of temperature measurement using the DC resistance value of the inductor and the characterization of the standard reported in [1]. Because this method is different than the used by the other participants then INTI decided to discard the L_7 measurements and participate in the comparison only with the L_5 and L_6 measurements. INMETRO decided to use the proposed method to determine the L_7 temperature using characterized values of R_0 = 8.543 25 Ω at 28.5 °C and a resistance temperature coefficient of 33.26 mΩ/°C.

After the third loop, the pilot laboratory repaired the L_7 sensor leads and recalibrated the sensor. A change of 0.5 mΩ in the R_0 constant of the sensor was found, representing a temperature difference of 1.5 mK, having an influence of 0.05 µH/H of inductance, so this effect was considered negligible and the new R_0 constant was used to determine the L_7 enclosure temperature for the third loop of the comparison.

For inductance measuring, the participants used different systems, described in the following paragraphs ordered by participation in the comparison. More detailed information can be found in Annex A.

CENAM – Mexico (Pilot Laboratory)

The pilot laboratory used a Three-Terminals Maxwell-Wien bridge optimized to measure low quality factor 10 mH inductors. The inductance measurement is performed using a current of 3.2 mA at 1 kHz, using as references one 10 nF capacitor and two 1 kΩ frequency-characterized resistors, calibrated using as reference the value of the national standard of capacitance, traced to capacitors maintained at BIPM, and the value of the national standard of electrical resistance maintained at CENAM with the reproduction of the Quantum Hall Effect, respectively [3]. The balance of the bridge includes an auxiliary Wagner balance.

NRC - Canada

NRC used a Four-Terminal co-axial pair Maxwell-Wien bridge applying to the inductor in almost all cases 6 mA, using as source of traceability:

- 1 kΩ, 10 kΩ, and 100 kΩ resistors traceable to Quantum Hall Resistance via NRC cryogenic current comparator bridge to NRC working standards of resistance. The frequency dependence of 1 kΩ, 10 kΩ, and 100 kΩ resistors are traceable to a 1 kΩ calculable resistor of the quadrifilar type.
- 10 pF and 1 nF capacitors calibrated using a substitution method with respect to one of the 10 pF primary standards fused silica capacitors traceable to BIPM capacitors.
- the source used to power the bridge was phase locked to the NRC 10 MHz frequency standard and is thus traceable to the NRC atomic clocks.

NIST - United States of America

For inductance measurements, NIST used a digital impedance bridge supporting LCR meter measurements. The digital impedance bridge measurements are traceable to the NIST calculable capacitor through calibrated capacitance standards using scaling within the digital impedance bridge. For 10 mH inductance measurements at 1000 Hz, they are used 25 Ω and 100 Ω ac-dc resistors calibrated at dc, as well as at 1000 Hz from scaling through 1 nF to 100 kΩ, 10 kΩ, 1 kΩ, and 100 Ω standards.

INTI - Argentina

A Maxwell-Wien bridge with Wagner arm, zero substitution was used by INTI. Traceability is obtained by means of two 1 kΩ resistors calibrated in terms of the reproduction of the Quantum Hall Effect, and capacitors calibrated using 10 pF fused silica capacitors traced to a 10 pF group of capacitors maintained at BIPM.

INMETRO - Brazil

INMETRO used a Maxwell-Wien bridge using as reference two resistors and one capacitor with value traceable to BIPM [4].

ICE - Costa Rica

A substitution method was used at ICE to measure inductance using an LCR bridge and a reference inductor. The method is based to know the LRC error before use it for measuring the unknown inductor, by using a reference inductor with value traced to METAS - Switzerland.

UTE - Uruguay

UTE used a four-arm alternating-current Owen Bridge with Wagner ground for measuring inductance in terms of capacitance, resistance and frequency [5] with traceability to PTB-Germany for Capacitance through a 1000 pF standard capacitor, BIPM for resistance through a 1 Ω Thomas resistor, and to UTE for frequency through a Cesium Atomic Clock.

The reported measurements and its analysis are described in the following section.

4.4. Measurements results

The measurements results of the comparison were obtained following different stages:

a) The NMI's individual reported measurements were corrected at a reference temperature, according the characteristics of the enclosures, in order to have comparability of measurements for each individual inductor.

b) With basis on the measurements of the pilot laboratory, it was determined a time-dependent reference value for each inductor, which is useful to have a common reference value between the measurements of inductors.

c) They were computed the differences between the reference value of each inductor and the NMI's corrected measurements. Using these differences, it was computed a combined difference for each NMI.

d) Finally, it was computed the Key Comparison Reference Value and equivalence using the combined difference using the combined difference from each NMI.

The details of the mentioned stages are described below.

4.4.1. Reported measurements and temperature corrections

After proceed to make any computation, all reported measurements were analyzed to detect possible invalid measurements or possible errors on transcription. In case, the technical contact was asked to confirm the reported data. The individual inductance official measurements reported by the participants are shown in figures 16, 17 and 18, expressed as deviation from the nominal value (DNV) in μH/H.

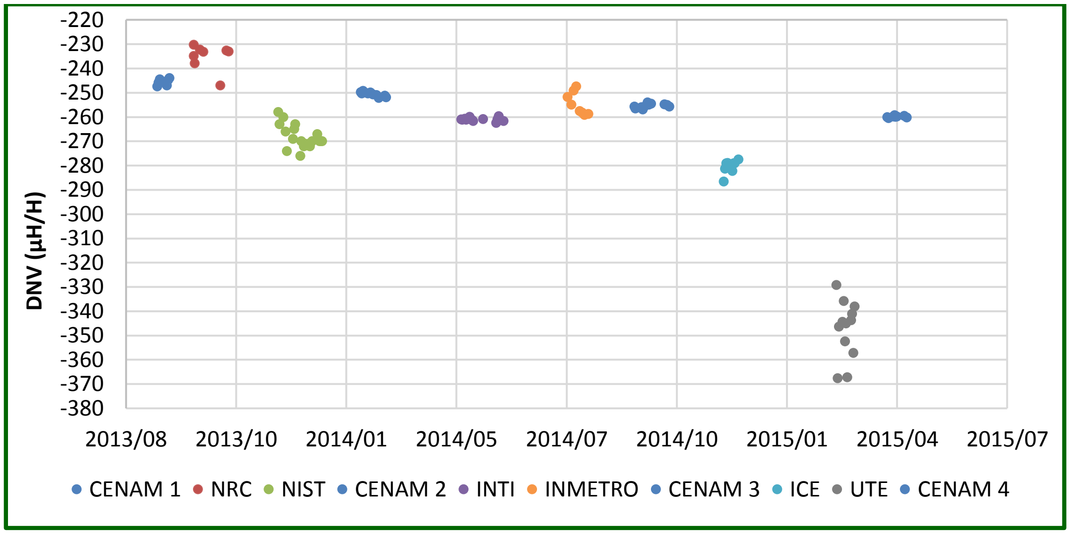

Figure 16 Individual inductance measurements reported for L_5.

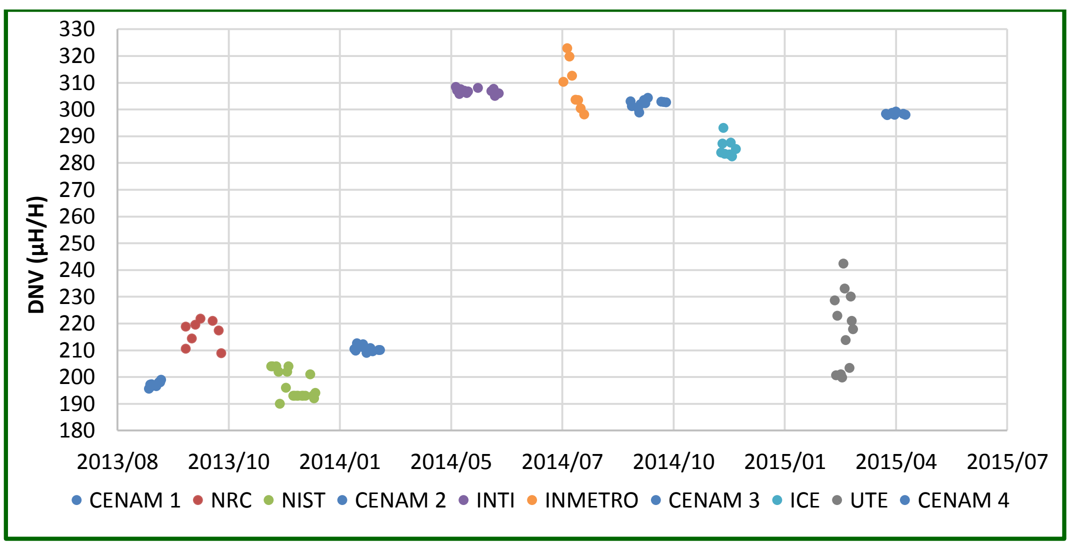

Figure 17 Individual inductance measurements reported for L_6.

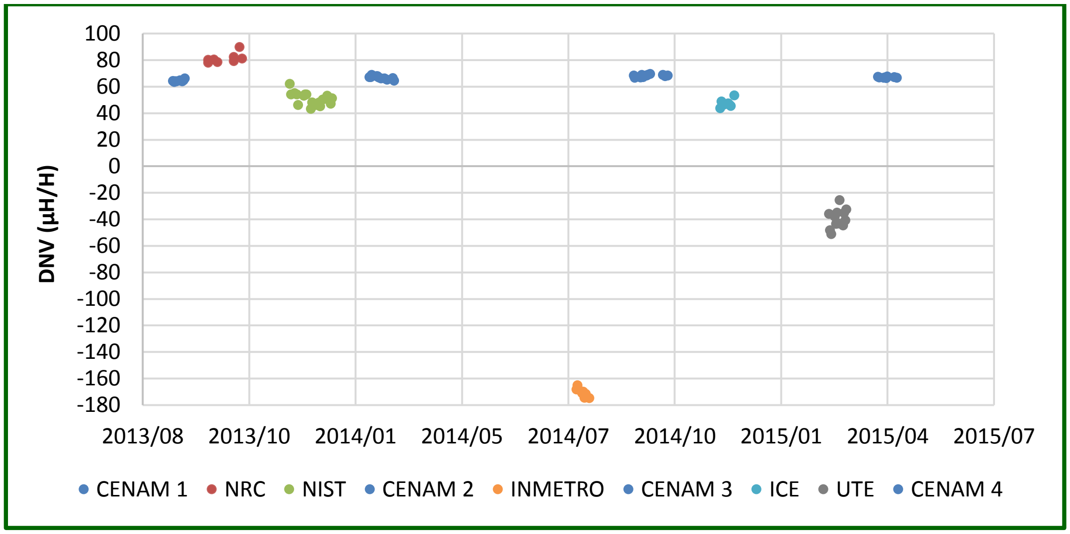

Figure 18 Individual inductance measurements reported for L_7.

All participants measured the temperature of the enclosures by means of the corresponding Pt100 sensor, but in the case of INMETRO, the temperature of the enclosure L_7 was determined by means of the DC resistance of the inductor, due the reasons explained in the section 4.3 of this report. The temperature reported for each enclosure can be observed in figures 19 to 22.

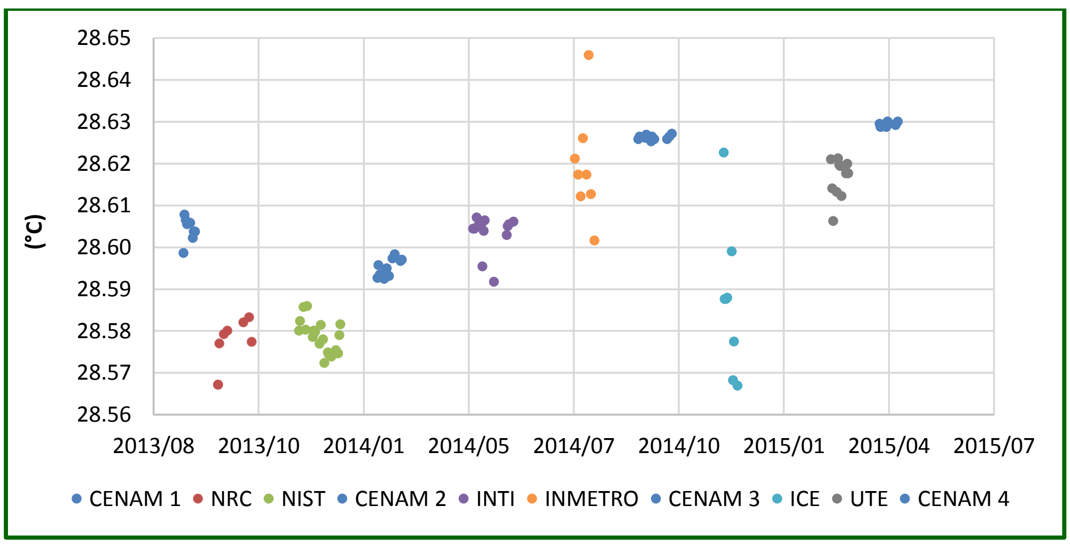

Figure 19 Temperature of the enclosure L_5.

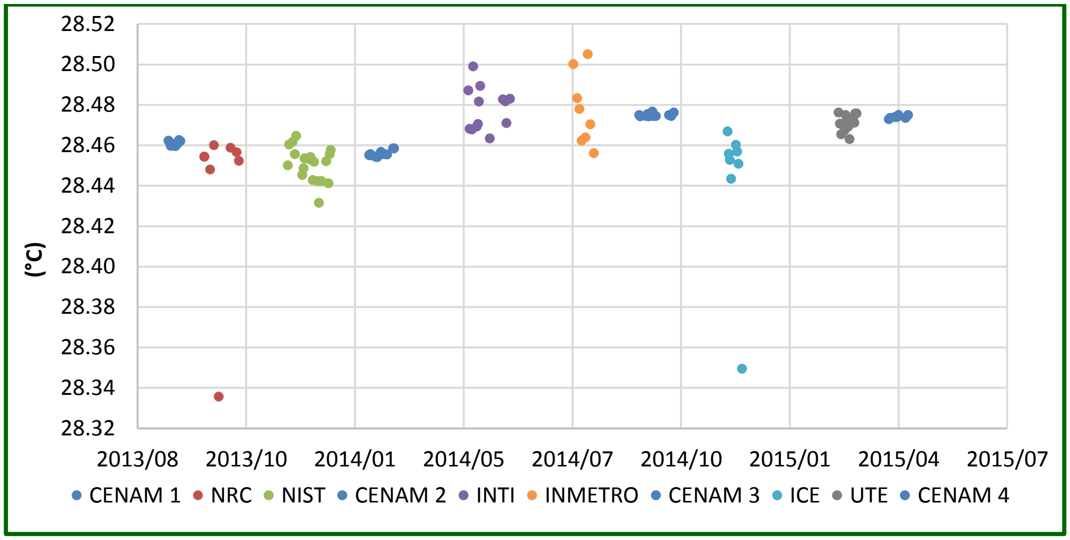

Figure 20 Temperature of the enclosure L_6.

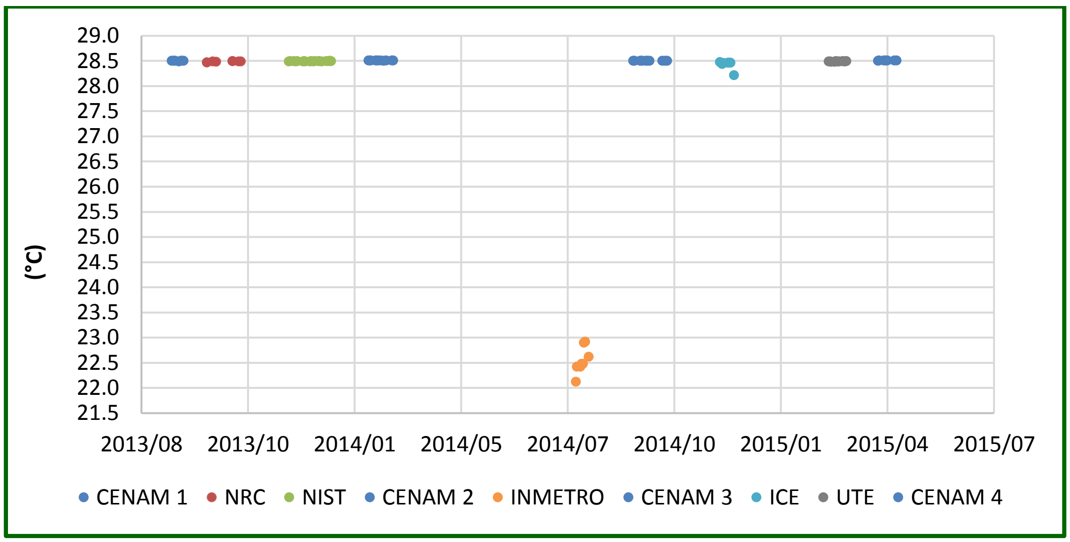

Figure 21 Temperature of the enclosure L_7.

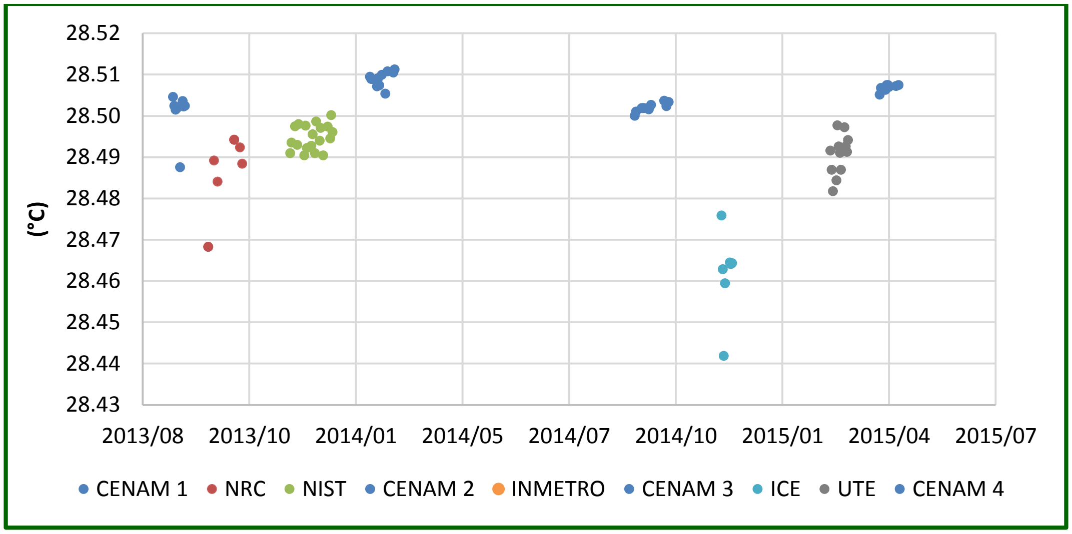

Figure 22 Temperature of the enclosure L_7 (excluding INMETRO).

As can be seen, for each enclosure the temperature was different along the comparison, so it was necessary to apply a temperature correction to the reported values in order to have comparability between them.

To perform this correction it was necessary to determine a reference temperature for each enclosure, which was determined by means of the average value of all participants rounded to two decimal digits, except for L_7, where the INMETRO measurements were excluded. Table 4 shows the determined reference temperature for each enclosure.

Table 4 Reference temperature of the enclosures.

Enclosure	Average Temperature
L_5	28.60 °C
L_6	28.46 °C
L_7	28.49 °C

The individual measurement results of the participants were corrected at the reference temperature of the corresponding enclosure, using the temperature coefficient of each inductor. The average applied correction was less than 1 µH/H for the most of the cases, except for the L_7 INMETRO measurement, which was in average 223.5 µH/H due the explained reasons before. The average of the applied corrections for each participant are listed in table 5.

Table 5 Average applied correction.

NMI	Enclosure L_5 (µH/H)	Enclosure L_6 (µH/H)	Enclosure L_7 (µH/H)
CENAM 1	-0.16	-0.05	-0.40
NRC	0.87	0.97	0.19
NIST	0.80	0.45	-0.18
CENAM 2	0.18	0.21	-0.71
INTI	-0.12	-0.88	---
INMETRO	-0.72	-0.84	223.5
CENAM 3	-0.98	-0.73	-0.45
ICE	0.48	0.87	2.22
UTE	-0.63	-0.55	-0.02
CENAM 4	-1.10	-0.68	-0.63

The standard uncertainty of the temperature corrections was:

0.37 µH/H for L_5
0.49 µH/H for L_6
0.38 µH/H for L_7

In case of the L_7 INMETRO measurements, the uncertainty of the temperature correction was 4.8 µH/H. In all cases, this uncertainty was considered as an additional type B contribution.

Using the corrected individual values, it was computed the mean corrected value for each participant for the corresponding traveling standard, which is listed in table 6, where the mean date is expressed in the 1900 date system. The uncertainties type A, B, coverage factor k and expanded uncertainty, for each case, are shown in tables 7 to 9. More detailed information can be found in Annex B.

Table 6 Mean corrected values.

NMI	Mean Date	Mean Date in 1900 Date System	ML_5 (µH/H)	ML_6 (µH/H)	ML_7 (µH/H)
CENAM 1	2013-09-01	41518	-245.7	197.2	63.9
NRC	2013-10-09	41556	-234.3	217.5	81.3
NIST	2013-12-24	41632	-267.5	197.1	50.3
CENAM 2	2014-02-20	41690	-250.4	210.6	65.9
INTI	2014-05-21	41780	-261.1	306.0	---
INMETRO	2014-08-10	41861	-255.3	308.1	52.7
CENAM 3	2014-10-08	41920	-256.4	301.5	67.5
ICE	2014-12-13	41986	-280.0	286.6	49.3
UTE	2015-03-19	42082	-348.0	217.3	-39.7
CENAM 4	2015-04-29	42123	-261.0	297.7	66.1

Table 7 Uncertainty components for L_5.

NMI	uA (µH/H)	uB (µH/H)	k	U (µH/H)
CENAM 1	0.4	5.5	2.0	11
NRC	1.9	11.1	2.3	26
NIST	4.5	21.1	2.0	43
CENAM 2	0.3	5.5	2.0	11
INTI	0.3	9.7	2.0	19
INMETRO	1.6	13.0	2.0	26
CENAM 3	0.3	5.5	2.0	11
ICE	1.0	16.4	2.0	33
UTE	4.0	40.1	2.1	85
CENAM 4	0.1	5.5	2.0	11

Table 8 Uncertainty components for L_6.

NMI	uA (μH/H)	uB (μH/H)	k	U (μH/H)
CENAM 1	0.4	5.5	2.0	11
NRC	1.7	11.1	2.3	26
NIST	4.5	21.1	2.0	43
CENAM 2	0.3	5.5	2.0	11
INTI	0.3	9.7	2.0	19
INMETRO	3.2	13.0	2.0	27
CENAM 3	0.5	5.5	2.0	11
ICE	1.0	16.4	2.0	33
UTE	4.0	40.1	2.1	85
CENAM 4	0.2	5.5	2.0	11

Table 9 Uncertainty components for L_7.

NMI	uA (μH/H)	uB (μH/H)	k	U (μH/H)
CENAM 1	0.3	5.5	2.0	11
NRC	1.3	11.1	2.3	26
NIST	4.5	21.1	2.0	43
CENAM 2	0.4	5.5	2.0	11
INTI	---	---	---	---
INMETRO	4.5	15.5	2.0	32
CENAM 3	0.3	5.5	2.0	11
ICE	1.0	16.4	2.0	33
UTE	4.0	40.1	2.1	85
CENAM 4	0.1	5.5	2.0	11

Figures 23 to 25 shows the graph for the values of table 6, were the error bars represent the expanded uncertainty.

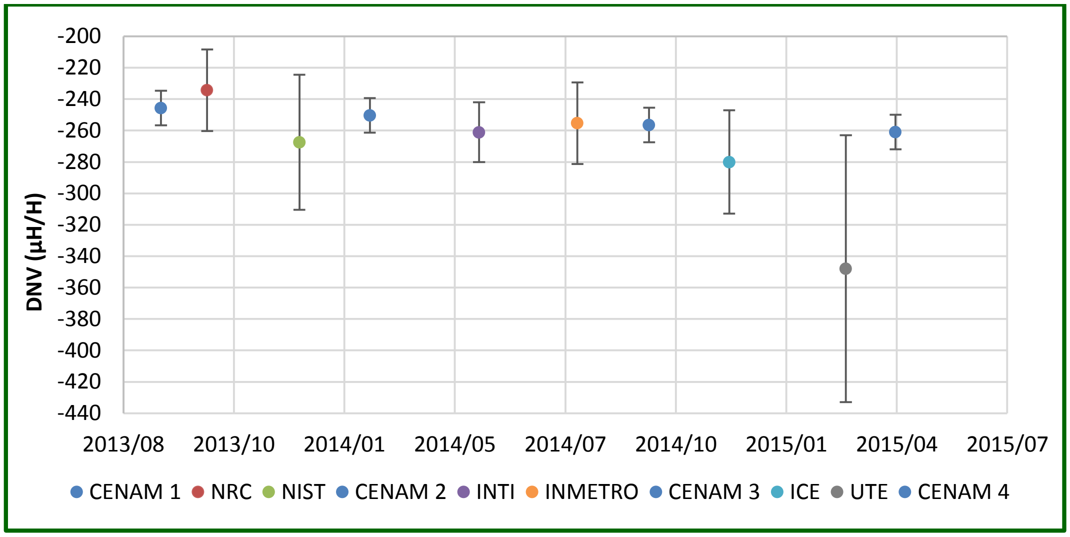

Figure 23 Mean corrected values for L_5.

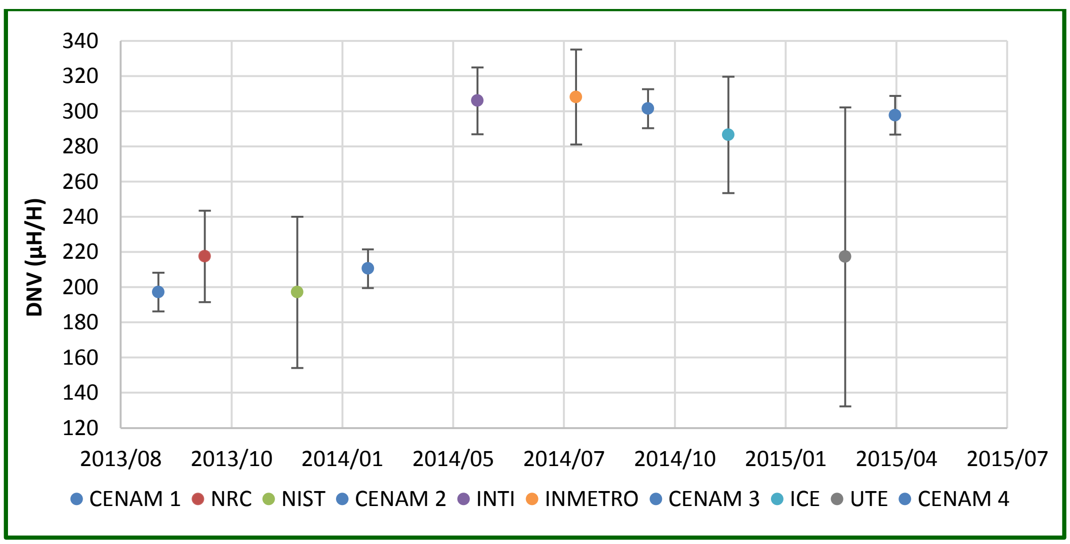

Figure 24 Mean corrected values for L_6.

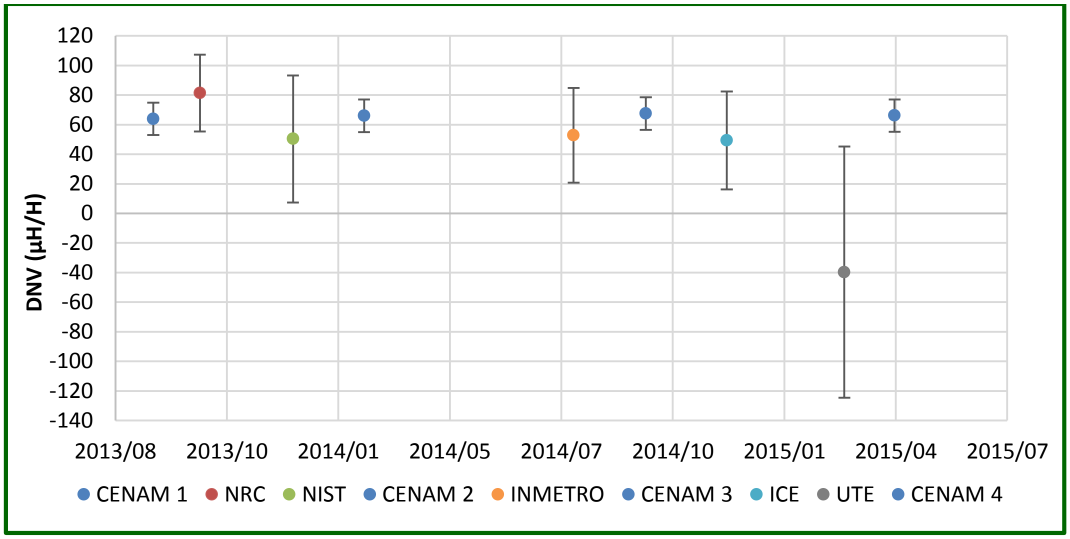

Figure 25 Mean corrected values for L_7.

4.4.2. Reference values

In order have a common reference value between the measurements of inductors, it was determined a reference value for each inductor, which is a time-dependent reference value calculated by means of a least-squares linear regression based on the pilot laboratory individual corrected measurements [6].

The reference values are straight lines fitted to the four CENAM mean corrected measurements. The fitted line was represented by means of the equation 1:

$$XL = Y_{LAV} + m\,(t - X_{CENAM\text{-}AV}) \tag{1}$$

where:

XL	is the value of the line in µH/H at the date t given in the 1900 Date System,
Y_{LAV}	is the value of line for the date t = X_{LAV} in µH/H,
m	is the slope of the line in µH/H per day,
t	is a date given in the 1900 Date System, and
$X_{CENAM\text{-}AV}$	is the average date for the CENAM measurements.

For the inductors L_5 and L_7, the obtained parameters of the fitted lines are shown in table 10.

Table 10 Parameters of the fitted lines.

Inductor	**XL_{AV} in 1900 Date System**	**m** (µH/H / day)	**YL_{AV}** (µH/H)
L_5	41813	-25.36×10^{-3}	-253.38
L_7	41813	3.93×10^{-3}	65.85

Figures 26 and 27 shows the fit of the lines to the measurements of L_5 and L_7 respectively.

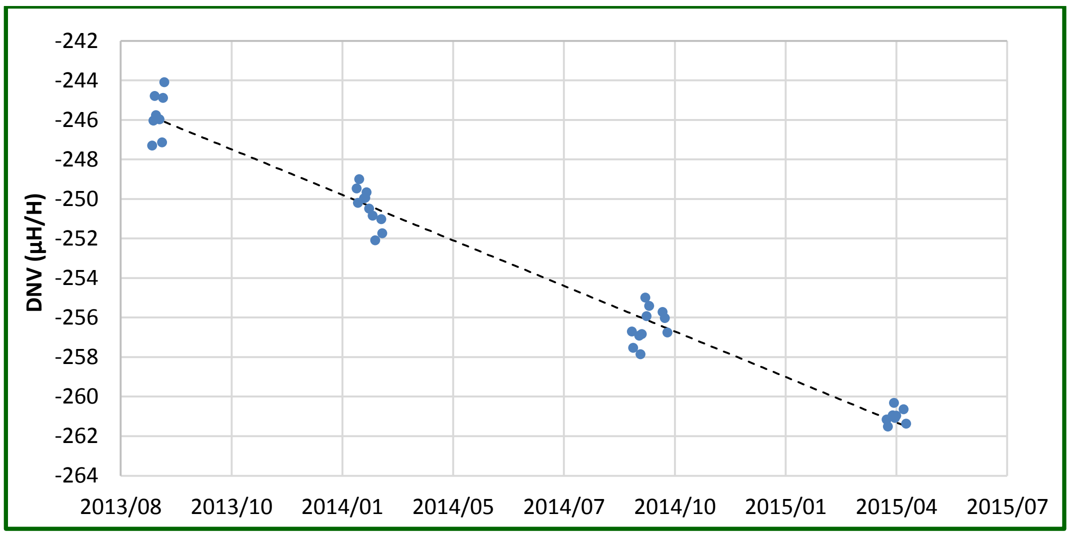

Figure 26 Linear regression for L_5.

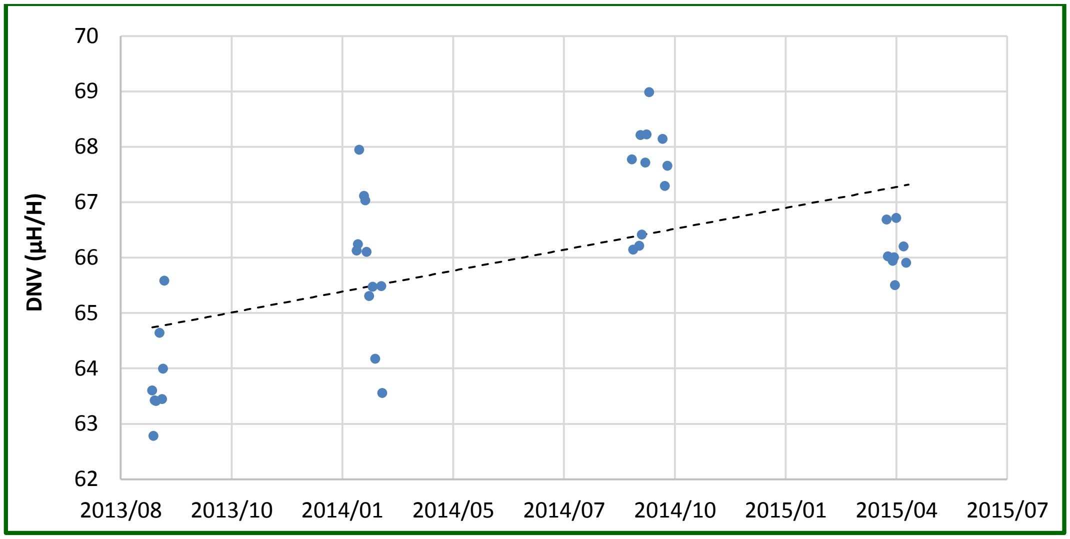

Figure 27 Linear regression for L_7.

As can be seen, the regression to L_5 fits very well all the measurements with deviations smaller than 2.1 µH/H around the line, and for L_7 the deviations don't exceed 2.6 µH/H, so it was considered that both reference lines are equally useful for the purpose of the comparison, considering the expanded uncertainties of the participants.

The residual standard deviation for the fitted lines was calculated according to equation 2:

$$\sigma r = \sqrt{\frac{\sum_{i=1}^{n}\left(M_{CENAM\text{-}i} - XL\right)^2}{n-2}} \tag{2}$$

where:

$M_{CENAM\text{-}i}$	is the ith CENAM corrected measurement,
XL	is the value of the fitted line for the dates of the ith CENAM corrected measurement, and
n	is number of times that CENAM measured each inductor.

The computed residual standard deviation for each fitted line is shown in table 11.

Table 11 Residual standard deviation for the fitted lines.

Inductor	σr
L_5	σr_5 = 0.325 μH/H
L_7	σr_7 = 1.296 μH/H

For the inductors L_5 and L_7 it was computed the value of its respective fitted line, XL_5 and XL_7, evaluated at the mean date of measurement of each participant. The corresponding standard uncertainty, u_{XL5} and u_{XL7}, was computed according to [7] using the equation 3:

$$u_{XL} = \sigma r \sqrt{1 + \frac{1}{n} + \frac{(X_i - X_{CENAM\text{-}AV})^2}{\sum_{j=1}^{n}\left(X_{CENAM\text{-}j}{}^2\right) - \frac{\left(\sum_{j=1}^{n} X_{CENAM\text{-}j}\right)^2}{n}}} \qquad (3)$$

where:

σr	is the residual standard deviation of the fitted line,
n	is number of times that CENAM measured each inductor,
X_i	is the mean date of measurement of the i^{th} participant,
$X_{CENAM\text{-}AV}$	is the average date for the CENAM measurements, and
$X_{CENAM\text{-}j}$	is the mean date of the j^{th} CENAM measurement.

The computed XL_5, XL_7, u_{XL5} and u_{XL7} values, for each NMI, are shown in table 12.

Table 12 Values of fitted lines corresponding to each NMI.

NMI	Mean Date in 1900 Date System	XL_5 (µH/H)	u_{XL5} (µH/H)	XL_7 (µH/H)	u_{XL7} (µH/H)
CENAM 1	41518	-245.90	0.42	64.69	1.67
NRC	41556	-246.86	0.41	64.84	1.62
NIST	41632	-248.79	0.39	65.14	1.54
CENAM 2	41690	-250.26	0.37	65.37	1.49
INTI	41780	-252.54	0.36	65.72	1.45
INMETRO	41861	-254.60	0.36	66.04	1.46
CENAM 3	41920	-256.09	0.37	66.27	1.48
ICE	41986	-257.77	0.38	66.53	1.53
UTE	42082	-260.20	0.41	66.91	1.64
CENAM 4	42123	-261.24	0.42	67.07	1.69

As explained before, the inductor L_6 suffered a big change during the transport from CENAM to INTI. In figure 11 it can be easily observed that the behavior of the inductor before the occurred change is different than the behavior after it, and additionally some other small changes occurred during the comparison.

Different evaluations of the information obtained from L_6 were intended in order to include the measurements of this inductor in the final results. It was tried:

- Make correction of the observed changes and fit a line to the corrected values.
- Use two different reference lines to describe the behavior of the inductor before and after the main change.
- Use the surveillance measurements reported by the participants to predict the value of the inductor during the stay at each NMI, and fit a line to the measurements and predictions.

Different problems arose from the mentioned evaluations, for instance not enough degrees of freedom for statistical estimation for interpolation or extrapolation, discrepancies or high residual deviations from linear trends. In all cases the evaluations produce an undesired contribution of standard uncertainty in the order of 10 µH/H, which is not acceptable for the purposes of the comparison, so it was decided to discard the measurements made to L_6 and support the comparison with the L_5 and L_7 inductors measurements.

4.4.3. Differences from the reference values

Having the reference value for the inductors L_5 and L_7 (table 12) and the NMI's corrected measurements (table 6), they were computed the differences D_i for each NMI according the equation 4:

$$D_i = ML_i - XL_i \tag{4}$$

where:

ML_i is the mean corrected value of the i[th] NMI, and
XL_i is the reference value corresponding to the i[th] NMI.

From these computed differences it was obtained only one combined difference D_C for each NMI. After analyzing the behavior of inductors and the linear trend of the measurements it was concluded and agreed that the most adequate way to compute D_C is using simply the average of the obtained differences according the equation 5:

$$D_{Ci} = \frac{D_{5i} + D_{7i}}{2} \tag{5}$$

where:

DC_i is the combined difference for the ith NMI, and

D_{5i} , D_{7i} are the differences for the i^{th} NMI for L_5 and L_7 respectively.

Considering that u_{XL5} and u_{XL7} represents in all cases a very small component of uncertainty, the expanded uncertainty of D_C for each NMI was computed using the equation 6, even for the pilot laboratory [8]:

$$UD_{Ci} = k_i \cdot \sqrt{\sum_{j=5,7} \left[\frac{uAi_j^{\,2} + uBi_j^{\,2} + u_{XLj}^{\,2}}{4} \right] + \frac{uBi_5 \cdot uBi_7}{2}} \qquad (6)$$

where:

UDC_i is the expanded uncertainty of the combined difference for the i^{th} NMI,

k_i is the coverage factor k reported by the i^{th} NMI, and

uAi_j, uBi_j are the uncertainties type A and B for the i^{th} NMI corresponding to the inductors L_5 and L_7.

The computed D_i, D_C and UD_C are shown in table 13, including the CENAM mean value, which will be considered as the best estimate for the pilot laboratory.

Table 13 Computed Di, D_C and UD_C.

NMI	D_5 (μH/H)	D_7 (μH/H)	D_C (μH/H)	UD_C (μH/H)
CENAM 1	0.20	-0.79	-0.3	11
NRC	12.56	16.46	14.5	26
NIST	-18.71	-14.84	-16.8	43
CENAM 2	-0.14	0.53	0.2	11
INTI	-8.56	---	-8.6	19
INMETRO	-0.70	-13.34	-7.0	29
CENAM 3	-0.31	1.23	0.5	11
ICE	-22.23	-17.23	-19.7	33
UTE	-87.80	-106.61	-97.2	84
CENAM 4	0.24	-0.97	-0.4	11
CENAM (Mean)	0.0	0.0	0.0	11

4.4.4. Key Comparison Reference Value and Equivalence

According to [9], linking results with the CCEM-K3 of this comparison won't be calculated until the new CCEM-K3 results are available, so it was used a Key Comparison Reference Value (KCRV) in order to compute equivalence.

The obtained D_C's were used to define the KCRV. According to the protocol, the KCRV should be computed considering measurements from those participants having independent realizations of the henry, whose uncertainty contribution to the KCRV is not a substantial part of the overall uncertainty. After an analysis of the results, it was recommended to define the KCRV using a weighted mean of the D_C's corresponding to all participants according the equation 7:

$$KCRV = \frac{\sum_{i=1}^{7} \left(w_i \cdot D_{Ci} \right)}{\sum_{i=1}^{7} w_i} \tag{7}$$

where:

w_i are the weights defined using the expanded uncertainty of the combined difference of the i[th] NMI,

$$w_i = \frac{1}{UD_{Ci}^{2}}$$

DC_i is the combined difference for the i[th] NMI.

For CENAM it was used only the mean value of the corresponding D_C's.

Regarding the KCRV uncertainty U_{KCRV}, it exists a correlation component originated in the fact that the capacitance value used by CENAM, NRC, INTI and INMETRO is traceable to the BIPM. The uncertainty contribution due this correlation component is lower than 1 µH/H, which was considered negligible, so the U_{KCRV} was calculated using the equation 8:

$$U_{KCRV} = \frac{1}{\sqrt{\sum_{i=1}^{7} w_i}} \tag{8}$$

The resulting value of the KCRV and its expanded uncertainty are:

KCRV = -3.4 µH/H **U_{KCRV} = 8.1 µH/H**

The degree of equivalence D_{KCRV} with the KCRV for each participant was computed using the equation 9:

$$D_{KCRVi} = D_{Ci} - KCRV \quad (9)$$

Because all participants are involved in the definition of the KCRV then the expanded uncertainty UD_{KCRV} was computed using the equation 10:

$$UD_{KCRVi} = \sqrt{UD_{Ci}^{2} - U_{KCRV}^{2}} \quad (10)$$

The computed D_{KCRV} and U_{KCRV} for each participant is listed in table 14.

Table 14 Computed D_{KCRV} and its uncertainty UD_{KCRV}.

NMI	D_{KCRV} (µH/H)	UD_{KCRV} (µH/H)
CENAM	3.4	7.4
NRC	17.9	24.7
NIST	-13.4	42.2
INTI	-5.2	17.2
INMETRO	-3.6	27.8
ICE	-16.3	32.0
UTE	-93.8	83.6

The graph of equivalence is shown in figure 28, where the error bars represent UD_{KCRV}.

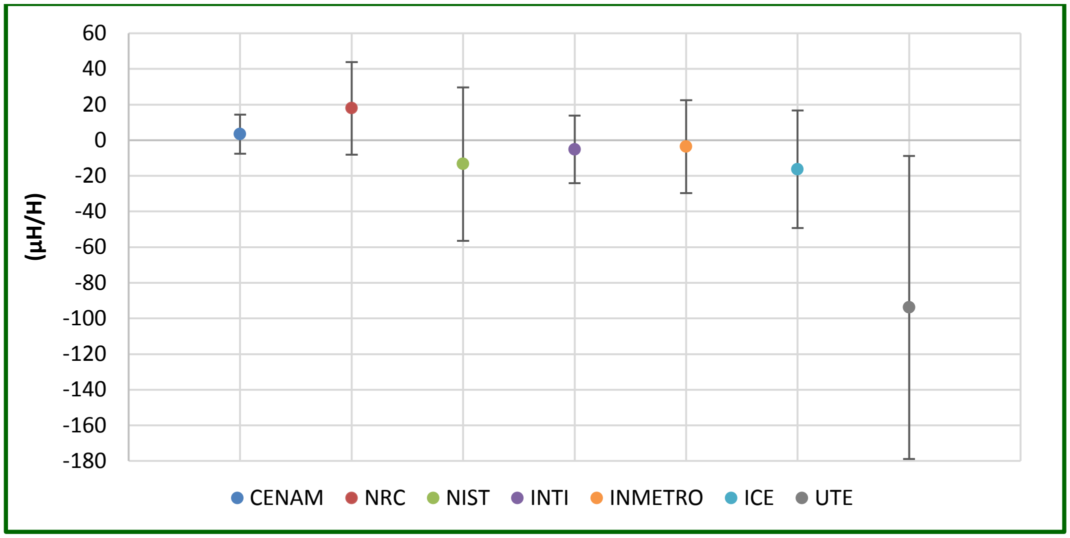

Figure 28 Computed D_{KCRV}.

The matrix of equivalence [10] containing the full set of degrees of equivalence between pairs D_{ij} of participants can be computed directly from the individual D_C according the equation 11.

$$D_{ij} = D_{Ci} - D_{Cj} \tag{11}$$

As explained, the existing correlation components of uncertainty between laboratories are negligible, so the uncertainty of each D_{ij} can be estimated using the equation 12.

$$UD_{ij} = \sqrt{UD_{Ci}^{2} + UD_{Cj}^{2}} \tag{12}$$

According to [9], linking results with the CCEM-K3 won't be calculated until the new CCEM-K3 results are available.

5. Conclusions

In accordance with the MRA objectives a Key Comparison of 10 mH Inductance Standards at 1 kHz was realized, obtaining as result the degree of equivalence of the measurement results of the seven participants.

During the transportation of the traveling standards very valuable information was obtained with the use of a Data Logger and surveillance measurements based on the measurement of inductance differences at each laboratory. Additionally, the use of temperature controlled enclosures, an appropriate transport case and previous characterization of the traveling standards was very important on the development of the comparison.

Different difficulties arose during the measuring stages, which were solved with the valuable help of the participants. Unfortunately, the measurements of one of the traveling standards was discarded, but thanks to the good behavior of the other two traveling standards the objectives of the comparison were satisfactorily accomplished.

For one participant, the temperature of one of the traveling standards was estimated using the DC resistance of the inductor, with the help of the previous characterization of the standard. This resulted in a good alternative of temperature measurement of inductors, which can be used in future inductance comparisons.

The results indicate good agreement among the most of the participants within their expanded uncertainties, which will be helpful to provide support for the participants' entries in Appendix C of the MRA.

The results need to be linked to the CCEM-K3. This will be done when the new CCEM-K3 results are available.

Acknowledgments

The author wish to express the more deep gratitude to the colleagues from the participating laboratories for their cooperation. Thanks to Marcel Cote, Andrew Koffman, Marcelo Cazabat, Renata de Barros e Vasconcellos, Blanca Isabel Castro, and Daniel Izquierdo, for their friendship and confidence expressed during this international metrology exercise. Thanks to Carlos Sánchez and Gregory Kyriazis for their valuable comments and advices during the process of review of the early versions of this document.

The author also acknowledges the valuable participation of CENAM colleagues. Thanks to Dr. René Carranza for his unconditional support to realize this important comparison, M.C. Felipe Hernández for his encourage, guidance and reviews to successfully follow up the development of the comparison, and Dr. David Avilés and M.C. Alepth Pacheco for their valuable advices and reviews.

References

[1] Moreno J. Angel, "Determinación de Coeficientes de Temperatura de Patrones de Autoinductancia", Simposio de Metrología 2014, http://www.cenam.mx/memorias/doctos/SM2014-056.pdf

[2] Snow Chester, "Formulas for Computing Capacitance and Inductance", National Bureau of Standards Circular 544, USA, 1954, p. 27.

[3] Moreno J. Angel, Hernandez Felipe, "Inductance Measurements At CENAM", CPEM 2012, Washington, USA, CPEM Digest, pp. 720-721.

[4] Sousa A. Q. L., Ogino L. M., Toth E., Rocha G. M., New Configuration For The Maxwell-Wien Bridge", CPEM 2004, London, England, CPEM Digest, pp. 595-596

[5] Slomovitz D., Faverio C., Izquierdo D., Spaggiari A., "A Simple Bridge For The Calibration Of Standard Inductors", VII SEMETRO, Brazil, Sep. 2007.

[6] Dziuba R. F., Jarrett D. G., "CCEM-K2 Key Comparison of Resistance Standards at 10 MΩ and 1 GΩ", NIST, USA, 2001, http://kcdb.bipm.org/appendixB/appbresults/ccem-k2/ccem-k2_final_report.pdf

[7] Natrella, Mary G., "Experimental Statistics" NIST Handbook 91, p 5.19.

[8] JCGM 100:2008, "GUM 1995 with minor corrections — Evaluation of measurement data — Guide to the expression of uncertainty in measurement", September 2008.

[9] 2012 SIM Electricity and Magnetism Metrology Working Group Meeting Minutes, July 07 2012.

[10] CIPM MRA-D-05 Version 1.5, "Measurement comparisons in the CIPM MRA", March 2014, http://www.bipm.org/utils/common/documents/CIPM-MRA/CIPM-MRA-D-05.pdf

Annex A
Measuring Systems

1. CENAM - Mexico (Pilot Laboratory)

CENAM used a Three-Terminals Maxwell-Wien bridge designed and optimized to measure 10 mH standard inductors with low quality factor at 1 kHz following classical theory, including a Wagner arm, according the following electrical circuit (shielding not shown).

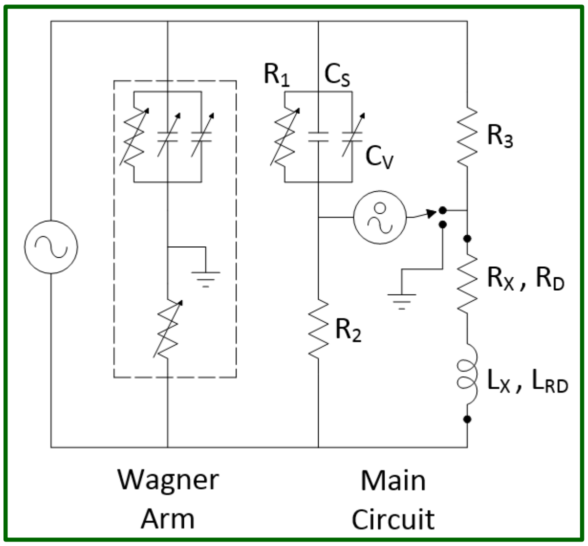

The capacitance reference C_S is a 10 nF ceramic capacitor with low temperature coefficient calibrated at the moment of the inductance measurement, the resistance references R_2 and R_3 are 1 kΩ resistors with low frequency dependence and low temperature coefficient. R_1 and C_V are used to balance the bridge using a two steps measurement technique:

1) Lx is connected to the bridge and the balance is obtained changing C_V and R_1. After the balance, C_V is measured (C_{V1}) using a high accuracy capacitance bridge.

2) L_X and C_S are removed and a variable resistor R_D, with very similar value to the resistance R_X of the inductor, is connected in place of L_X. The balance is obtained changing C_V and R_D only, and C_V is measured again (C_{V2}).

Considering parasitic impedances in the bridge, the value of L_X is calculated using the following equation:

$$L_X = R_2 \cdot R_3 \cdot (C_S + C_{V1} - C_{V2}) + C_S \cdot (R_2 \cdot R'_3 + R_3 \cdot R'_2) + L_{RD}$$

where R'_2 and R'_3 are internal resistances connecting R_2 and R_3 in the bridge respectively, and L_{RD} is the inductance of R_D.

The inductance measurement is performed using a current of 3.2 mA at 1 kHz. The value of the capacitances is known in terms of the national standard of capacitance, traced to capacitors maintained at BIPM, and the value of the resistors is known in terms of the national standard of electrical resistance maintained at CENAM with the reproduction of the Quantum Hall Effect.

2. NRC - Canada

NRC used a four terminal co-axial pair Maxwell-Wien Bridge. The schematic of the bridge is (equalizers not shown):

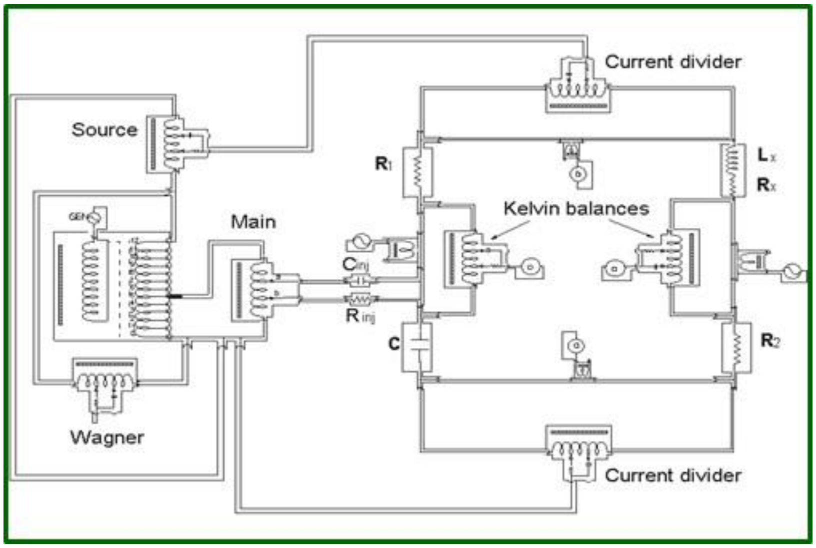

In the measurement of a 10 mH inductor, the reference capacitor C had a value of 1 nF, the resistors R_1, R_2 and R_{inj} were equal to 10 kΩ and 1 kΩ, and 100 kΩ, respectively. The resistors are composed of three sections. Two equal resistances connected in series and a variable capacitor connected from the junction of the two resistors to the case enclosing the resistors. For the 1 kΩ resistor it was necessary to use a small capacitance in series with the variable capacitor. The reactances of the 10 kΩ and 100 kΩ resistors could be minimized by adjusting the variable capacitor while measuring the capacitance of the resistor using an Andeen-Hagerling 2700A capacitance bridge. The reactance of the 1 kΩ resistor was minimized while comparing it to the 10 kΩ resistor using a four terminal 10:1 ac ratio bridge. The frequency dependence of the real part of their impedances was measured using a quadrifilar calculable resistor. The difference between the dc measurement and the 1 kHz measurement, in each case, was found to be less than 0.2 μΩ/Ω.

In practice, two measurements are made to minimize the effect of the residual inductance of the bridge itself. In the first measurement the unknown inductor is measured and in the second measurement a short is applied to the four terminals of the inductor arm of the bridge through a four terminal to two terminal adaptor. The short is constructed as a copper plate 5 cm by 5 cm, approximately 1 cm in thickness with two holes drilled the appropriate distance apart to accept the banana plugs of the adaptor. The short has an inductance calculated to be approximately 7 nH. In the second measurement, the capacitance of the 1 nF capacitor C is reduced to a negligibly small value, without modifying the outer coaxial-cable connections, by connecting a series adaptor having an open inner conductor. The 1 nF capacitor arm, in series with the adaptor has a capacitance of only a few aF's. Given the two measurements, the inductance of the unknown inductor can be calculated from:

$$Z_L = Z_{R_1} Z_{R_2}\left(\frac{1}{Z_c} + \frac{\alpha}{Z_{Cinj}} + \frac{\beta}{Z_{Rinj}}\right) - Z_{R_1} Z_{R_2}\left(\frac{1}{Z_{C0}} + \frac{\alpha o}{Z_{Cinj}} + \frac{\beta o}{Z_{Rinj}}\right)$$

The inductance and ac resistance can then be calculated using:

$$L_X = \frac{\mathrm{Im}(Z_L)}{\omega} - \frac{\mathrm{Im}(Z_{Lo})}{\omega} \qquad\qquad R_X = \mathrm{Re}(Z_l)$$

where:

Z_L, Z_{Lo}	Impedance of the device under test and impedance of a short-circuited bridge respectively.
L_x	Inductance of the device under test.
Z_{R1}, Z_{R2}, Z_{Rinj}	Impedances of 10 kΩ, 1 kΩ and 100 kΩ resistors with adjustable reactances.
Z_C, Z_{Cinj}	Impedances of a 1 nF capacitor and a 10 pF injection capacitor.
Z_{C0}	Impedance of a 1 nF capacitor with open circuit adaptor (assumed to be 0 pF).
α, αo	Main IVD dial settings for the in-phase (inductance) balance and short balance marked as "a" and "b" in the schematic)..
β, βo	Main IVD dial settings for the quadrature (resistance) balance and a short-circuited bridge balance .

Corrections

There are three corrections applied to the measurement result.

1) The correction due to the inductance of the shorting plate. As mentioned above this inductance is approximately 7 nH or 0.7 µH/H with respect to 10 mH. Therefore a correction of -0.7 µH/H should be applied to the measurement result.

2) The other error of consequence is due to the term:

$$Z_{R_1} Z_{R_2} \left(\frac{\beta}{Z_{Rinj}} \right)$$

Let:

$$Z_{R_1} = R_1 + jX_1, \quad Z_{R_2} = R_2 + jX_2 \quad \text{and} \quad Z_{R_{inj}} = R_{inj} + jX_{inj}$$

where

X_1, X_2, X_{inj} Reactances of the 10 kΩ, 1 kΩ and 100 kΩ resistors

Expanding this equation and dividing the imaginary part by ω we find that the contribution to the inductance is:

$$L_{error} = \frac{\beta \left[R_1 R_{inj} X_2 + R_2 R_{inj} X_1 - R_1 R_2 X_{inj} + X_1 X_2 X_{inj} \right]}{\omega (R^2{}_{inj} + X^2{}_{inj})}$$

The last term is of no significance, however the first three terms are. The first two are of the same sign and the third of the opposite sign. Consider for example if β=0.08, X2 =1 Ω, X1=0.1 Ω and Xinj =10 Ω the first two terms would cause an error of 13 µH/H each with respect to 10 mH (i.e. 26 µH/H in total) and the third term would cause an error of -13 µH/H. Thus a total error of +13 µH/H. The resistors were measured to have the following reactances: X2 =0.001 Ω, X1=0.001 Ω and Xinj =0.73 Ω. The error is calculated to be -0.8 µH/H with respect to 10 mH. The uncertainty of this correction is large due to the large standard deviations of the measurements of the reactances. In fact it is the largest uncertainty. Therefore a correction of +0.8 μH/H should be applied to the measurement result.

Since the correction for the short and that due to the reactances of the resistors are of opposite sign and are approximately the same no corrections are made to the measurement result.

3) Correction due to temperature. Since the measured variations of the temperatures of the enclosures (standard deviation of the mean of all individual enclosure temperatures) were less than 20 mK (i.e. <1 μH/H) and were normally distributed, no attempt to correct the inductance measurements to a particular temperature was made. Therefore the uncertainty due to temperature was omitted in the uncertainty budget. The final result applies to the measured inductance at the average temperature stated. Any variations in inductance due to variations in temperature are assumed to appear in the variance of the inductance measurements. If the pilot laboratory decides to normalize all the results of the participant laboratories to a temperature significantly different from that stated in the final result, it is presumed that the pilot laboratory will give each participant the opportunity to modify their respective uncertainties to take into account this effect.

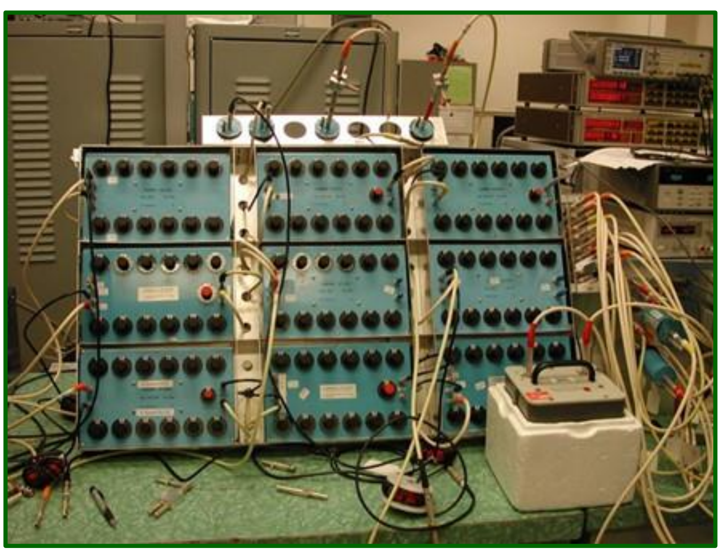

3. NIST - United States of America

The NIST used a Digital Impedance Bridge (DIB), which is a general-purpose ac bridge used to compare two, 4-terminal-pair (4TP) impedances with magnitudes between 0.1 Ω and 300 kΩ and phases between 0 and 360 degrees. It operates at frequencies from 10 Hz to 50 kHz with a best-case Type-B measurement uncertainty of 5×10^{-6} (1-σ) for 1:1 impedance ratios at 1 kHz.

A simplified diagram of the DIB is shown below, where V_1 and V_2 are programmable voltage sources applied to Z_1 and Z_2, respectively, producing currents I_1 and I_2 (all quantities are complex). The network of 1:1 current-comparator T_1 with tuned voltage detector D_5 is used to determine the condition when I_1 and I_2 are equal in magnitude and opposite in phase.

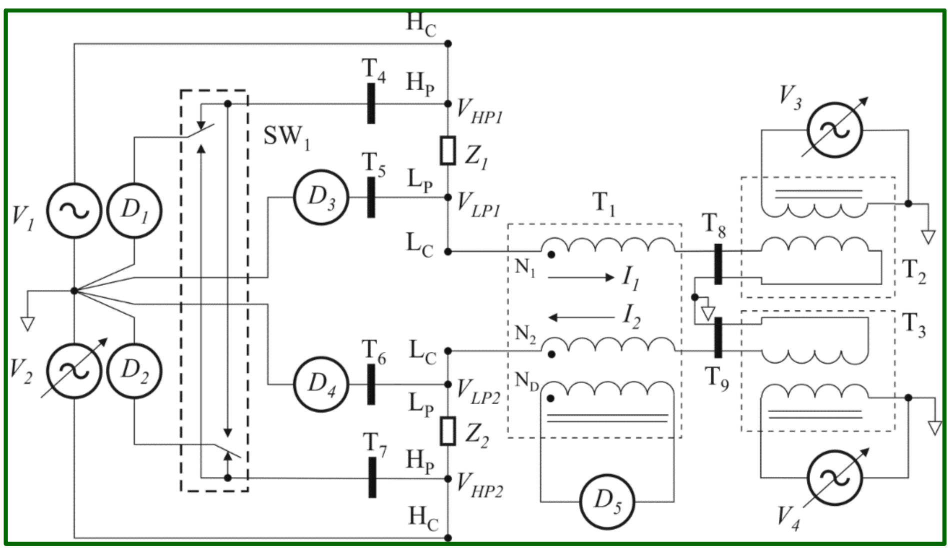

The N_D detection winding of T_1 consists of approximately 300 turns of #30 formvar magnet wire wound in a single-layer, bootlace fashion on a supermalloy toroidal core with reversals at ¼ and ¾ turns around the circumference of the core. A 1 mm copper electrostatic shield surrounds the detection winding. The 100-turn N_1 and N_2 ratio windings of T_1 are comprised of a twisted bundle of 12 wires wound 100 times in a bootlace fashion over the electrostatic shield with reversals at ¼ and ¾ turns around the circumference of the core. The magnetic errors between these two windings has been kept below $2x10^{-6}$ at 1 kHz by randomly selecting 6 of the wires in parallel for the N_1 and the remaining 6 in parallel for the N_2 winding, thereby eliminating the need for magnetic shielding between the ratio and detection windings. The sensitivity of T_1 is adequate to resolve impedance ratio differences below $1x10^{-6}$ at 50 Hz for impedance magnitudes below 300 kΩ. Programmable voltage sources V_3 and V_4 are used in conjunction with isolation transformers T_2 and T_3 and tuned detectors D_3 and D_4 to drive the low-potential terminals, V_{LP1} and V_{LP2}, respectively, of Z_1 and Z_2 to a null condition.

All interconnections between the various bridge components are coaxial (Not shown in the diagram). The effects of ground-loop induced bridge errors are minimized using coaxial current equalizers T_4-T_9.

The ratio and phase relationship between the high-potential terminals, V_{HP1} and V_{HP2} of Z_1 and Z_2, respectively, is determined using a set to two, commercially-available, high-accuracy, sampling digital voltmeters (DVMs), D_1 and D_2. The static phase error between D_1 and D_2 is measured and cancelled in software using channel-reversing switch SW_1. The 20 MHz time-base references for the D_1 and D_2 DVMs and the D_3-D_5 tuned null detectors are supplied from the V_1-V_4 signal generation hardware, thereby minimizing leakage effects associated with the FFT-based amplitude/phase estimation routines.

When the bridge is balanced, the relationship between the impedances is given by:

$$Z_2 = Z_1 \frac{V_{HP2}}{V_{HP1}}$$

For 10 mH inductance measurements at 1 kHz, Z_1 consists of a 100 Ω resistor with known magnitude and phase errors, as determined using a resistance bootstrap calibration procedure from 100 Ω to 100 kΩ, and a final comparison of the 100 kΩ to a calibrated, 1 nF, gas-dielectric capacitance standard. The combined uncertainty of the bridge, bootstrap, and 100 Ω to 10 mH comparison measurements is estimated to be below $2x10^{-5}$ (1-σ) at 1 kHz.

The bridge instrumentation is software-controlled using both USB and IEEE-488 buses by a library of LabVIEW virtual instruments (VIs) running on a host computer.

4. INTI - Argentina

The used method and measurement System by INTI was a Maxwell-Wien Bridge with Wagner arm, zero substitution. The diagram of the Bridge is:

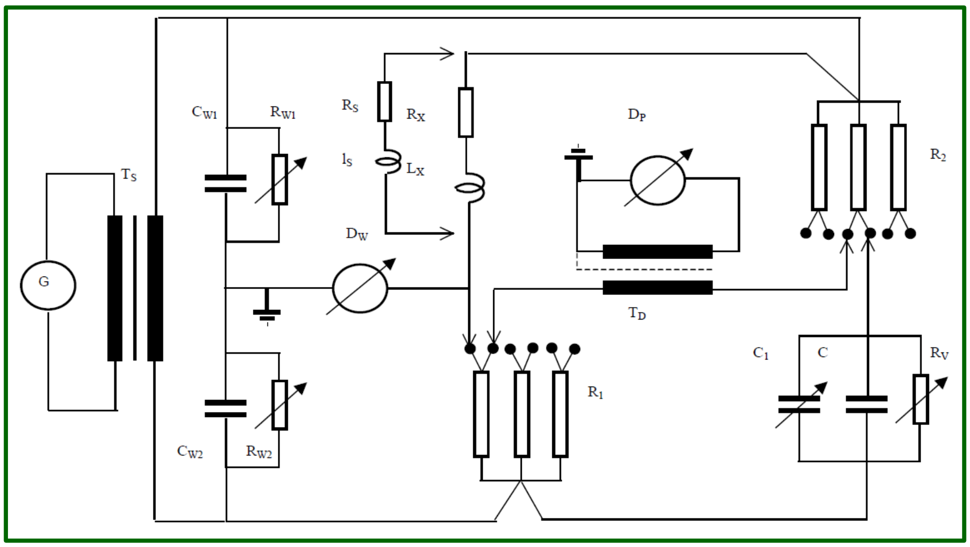

References:

R_1, R_2:	Resistances of the mean bridge.
C:	Mean capacitor.
C_1 (C'_1):	Balance precision capacitor (first and second measure respectively).
R_V:	Resistor to balance R_X and R_S.
R_X:	Series resistance of the inductor.
R_S:	Substitution resistance.
l_S:	Substitution inductance.
D_P, D_W:	Mean and Wagner detectors respectively.
C_{W1}, C_{W2}, R_{W1}, R_{W2}:	Wagner components.
T_S:	Isolation transformer.
G:	Power source.
T_D:	Detector transformer.

The value of the inductor to be measured is determined by means of:

$$L_X = \left[R_1R_2(C + C_1) + l_S - R_1R_2C'_1 - 4\pi^2 f^2 R_1{}^2 R_2{}^2 C^2 C_0\right]\left[1 \pm k\Delta t\right]$$

5. INMETRO - Brazil

INMETRO uses a Maxwell-Wien Bridge to calibrate de 1482-H Standard Inductors, at 1 kHz.

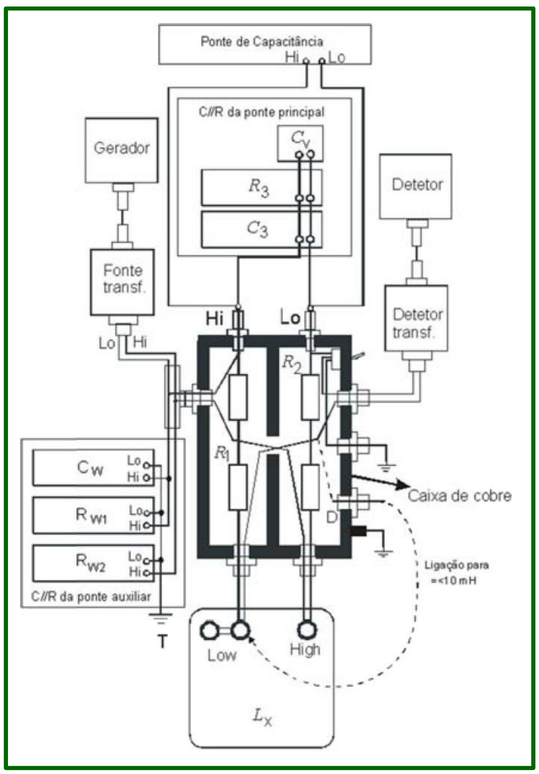

The value of the inductance of the standard inductor is related to the resistance and capacitance units by the mathematical relation:

$$L = R_1R_2C$$

where R_1 and R_2 are the resistances and C is the capacitance. INMETRO reference standards of both resistance and capacitance are traceable to BIPM.

6. ICE – Costa Rica

ICE used a substitution method to calibrate the inductance standard, which base is to know the LRC error before use it for measuring both the standard and the unknown inductor, by using a reference inductor. This process allows to know the LRC correction, which will be apply to the unknown inductor measurement.

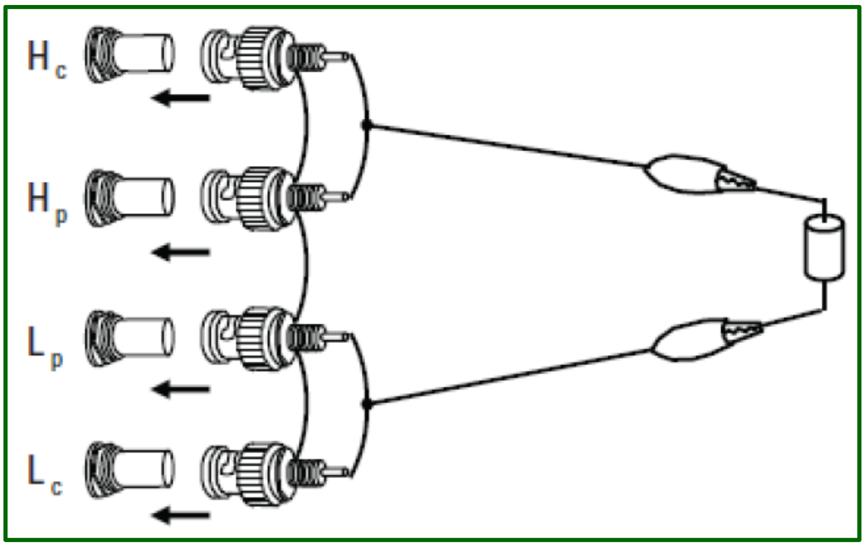

The minimum configuration set – up in the LRC Meter is:

FUNC: Ls – Q	(in order to obtain a better resolution, the LRC meter should be configure in the ΔABS function, where ΔABS = X – Y, X: Unknown measurement and Y: Reference Value).
FREQ: 1.000 kHz	
LEVEL: 1.000 V	
RANGE:	(Verify the LRC range where the measurements indicate the less variation between the readings).
BIAS: 0.000 V	

INTEG: LONG
AVG: 8 (minimum value)
CABLE: 0 m (this length will vary in accordance with the used cable)

7. UTE – Uruguay

A four-arm alternating-current Owen Bridge for measuring inductance in terms of capacitance, resistance and frequency was used by UTE. This bridge uses two voltage sources (both low-terminal grounded), to get the Wagner ground. A balance is made by means of a variable resistor and a variable capacitor, in parallel. The other arms are formed by: standard capacitor, fixed resistor, and unit under test. The inductance value is obtained as result of the following equation:

$$L = \left(\frac{R_V \cdot R \cdot C}{1 + (R_V \cdot C_V \cdot \omega)^2} \right) (1 + D \cdot R_V \cdot C_V \cdot \omega) - L_C$$

where:

R_V	Variable Resistor
R	Fixed Resistor
C	Fixed Capacitor
C_V	Variable Capacitor
L_C	Bridge residual Inductance
w	Frequency
D	Variable Capacitor Dissipation

Annex B
Uncertainty Budgets

1. CENAM - Mexico (Pilot Laboratory)

Uncertainty Component	***PDF / Eval. Type***	***Relative Contribution (µH/H)***
Repeatability (maximum observed)	Normal, A	0.46
Value of R_2	Normal, B	2.50
Stability of R_2	Rectangular, B	2.31
Value of R_3	Normal, B	2.50
Stability of R_3	Rectangular, B	2.31
Value of C_S	Normal, B	1.35
Value of C_{V1}	Rectangular, B	0.06
Resolution of C_{V1}	Rectangular, B	0.03
Value of C_{V2}	Rectangular, B	0.06
Resolution of C_{V2}	Rectangular, B	0.03
Value of R'_2	Rectangular, B	0.28
Value of R'_3	Rectangular, B	0.28
Value of L_{RD}	Normal, B	1.73
Mathematical Model and Bridge Balance	Normal, B	1.33
Combined Type A relative contribution:		**0.46**
Combined Type B relative contribution:		**5.47**
Combined relative standard uncertainty:		**5.49**
Coverage factor k (for a 95.45 % confidence level):		**2.0**
Expanded relative uncertainty:		**11**

2. NRC - Canada

Uncertainty Component	*PDF / Eval. Type*	*Relative Contribution (µH/H)*
$L(R_1)$ resistance of R_1 10 kΩ	Rectangular, B	2.0
$L(R_2)$ resistance of R_2 1 kΩ	Rectangular, B	2.0
L(C) capacitance of C	Rectangular, B	2.0
$L(C_{inj})$ capacitance of C_{inj}	Rectangular, B	0.6
Non-zero auxiliary balances	Rectangular, B	2.3
Additional capacitance introduced by 4-terminal to 2-terminal adapter between inductor terminals	Rectangular, B	0.6
Unequalized currents between inner and outer conductors	Rectangular, B	2.0
Uncertainty of the correction due to the inductance of the short	Rectangular, B	0.6
Uncertainty of the correction due to the reactances of R_1, R_2 and R_{inj}	Rectangular, B	10
Standard deviation of the mean of the L_0 measurements	Normal, A	2.0
Typical standard deviation of the mean of individual measurements of L	Normal, A	0.3
Standard deviation of the mean of all the measurements of L	Normal, A	1.9
Combined Type A relative contribution:		**2.8**
Combined Type B relative contribution:		**11.1**
Combined relative standard uncertainty:		**11.43**
Coverage factor k (for a 95.45 % confidence level):		**2.3**
Expanded relative uncertainty:		**25.8**

3. NIST - United States of America

Uncertainty Component	*PDF / Eval. Type*	*Relative Contribution (µH/H)*
Reference Capacitor	Normal, B	3.0
Impedance Bridge	Rectangular, B	21
Short-term Drift	Normal, A	4.5
Combined Type A relative contribution:		**4.5**
Combined Type B relative contribution:		**21.1**
Combined relative standard uncertainty:		**21.5**
Coverage factor k (for a 95.45 % confidence level):		**2**
Expanded relative uncertainty:		**43**

4. INTI - Argentina

Uncertainty Component	*PDF / Eval. Type*	*Relative Contribution (µH/H)*
Resistor 1 (R_1)	Rectangular, B	4.04
Resistor 2 (R_2)	Rectangular, B	4.04
Mean Capacitor (C)	Normal, B	7.00
Precision Capacitor read. 1 (C_1)	Rectangular, B	1.73
Precision Capacitor read. 2 (C_2)	Rectangular, B	1.73
Zero subst. Inductor (ls)	Rectangular, B	2.31
Temperature coefficient (k)	Rectangular, B	0.04
Temperature correction (Dt)	Normal, B	0.50
Frequency (f)	Rectangular, B	0.00
Residual capacitance of the unknown branch (C_0)	Rectangular, B	0.05
Repeatability	Normal, A	0.30
Combined Type A relative contribution:		**0.30**
Combined Type B relative contribution:		**9.66**
Combined relative standard uncertainty:		**9.66**
Coverage factor k (for a 95.45 % confidence level):		**2.0**
Expanded relative uncertainty:		**19.4**

5. INMETRO - Brazil

Uncertainty Component	*PDF / Eval. Type*	*Relative Contribution (μH/H)*
Capacitance Standard Calibration	Normal, B	10
Capacitance Standard History	Rectangular, B	4.2
Resistance Standard Calibration (R_1)	Normal, B	0.43
Resistance Standard AC Correction (R_1)	Rectangular, B	2.9
Resistance Standard Calibration (R_2)	Normal, B	0.49
Resistance Standard AC Correction(R_2)	Rectangular, B	2.9
Temperature Dependence (L_X)	Rectangular, B	5.8
Repeatability (L_5)	Normal, A	1.6
Repeatability (L_6)	Normal, A	3.2
Repeatability (L_7)	Normal, A	1.1
Combined Type A relative contribution (L_5):		**1.6**
Combined Type A relative contribution (L_6):		**3.2**
Combined Type A relative contribution (L_7):		**1.1**
Combined Type B relative contribution:		**13**
Combined relative standard uncertainty:		**13**
Coverage factor k (for a 95.45 % confidence level):		**2.0**
Expanded relative uncertainty:		**26**

6. ICE – Costa Rica

Uncertainty Component	*PDF / Eval. Type*	*Relative Contribution (µH/H)*
Repeatability in the measurement of Lx	Rectangular, B	1.2
Resolution in the measurement of Lx	Rectangular, B	0.0
Lx value	Normal, A	1.0
Standard Calibration Certificate	Normal, B	11.5
Standard Stability	Rectangular, B	9.8
repeatability in the measurement of the standard	Rectangular, B	1.7
Resolution in the measurement of Standard	Rectangular, B	0.0
Temperature Coefficient of the Standard	Rectangular, B	4.5
Temperature of the standard	Rectangular, B	3.5
Temperature Coefficient of the Lx	Rectangular, B	0.0
Temperature of Lx	Rectangular, B	2.2
Combined Type A relative contribution:		**1.0**
Combined Type B relative contribution:		**16.4**
Combined relative standard uncertainty:		**16.5**
Coverage factor k (for a 95.45 % confidence level):		**2**
Expanded relative uncertainty:		**33**

7. UTE – Uruguay

Uncertainty Component	***PDF / Eval. Type***	***Relative Contribution (µH/H)***
Variable Resistor Measurement δRV	Normal	29.0
Variable Resistor Resolution δRVi	Rectangular	5.6
Fixed Resistor Measurement δR	Normal	5.0
Fixed Capacitor Value δC	Normal	5.0
Capacitance Value variation due Temperature δC_T	Rectangular	3.0
Variable Capacitor Measurement δCV	Normal	8.6
Bridge residual Inductance δLc	Rectangular	17.3
Frequency Measurement δw	Normal	0.0
Variable Capacitor Dissipation Measurement δD	Normal	1.4
Inductance Value variation due Temperature δLt	Rectangular	17.3
Combined Type A relative contribution:		**4.0**
Combined Type B relative contribution:		**40.1**
Combined relative standard uncertainty:		**40.3**
Coverage factor k (for a 95.45 % confidence level):		**2.1**
Expanded relative uncertainty:		**85**